Documentation – User's Guide

Sentinel-1 processing with GAMMA software

Including an example of Sentinel-1 SLC co-registration and differential interferometry

GAMMA REMOTE SENSING

Version 1.1 – May 2015

GAMMA *Remote Sensing AG, Worbstrasse 225, CH-3073 Gümligen, Switzerland*
tel: +41-31-951 70 05, fax: +41-31-951 70 08, email: gamma@gamma-rs.ch

Table of contents

List of acronyms

DEM	Digital Elevation Model
DIFF&GEO	Differential Interferometry And Geocoding Software
ESA	European Space Agency
IPTA	Interferometric Point Target Analysis
ISP	Interferometric SAR Processor
IWS	Interferometric wide-swath mode
LAT	Land Application Tools
MLI	Multi-Look Intensity
MSP	Modular SAR Processor
PRF	Pulse Repetition Frequency
SAR	Synthetic Aperture Radar
S1	Sentinel-1
SLC	Single Look Complex
SRTM	Shuttle Radar Topography Mission
TOPS	Special SAR acquisition mode of Sentinel-1 [3]

Change record

V1.0 – Oct. 2014	Initial version
V1.1 – May 2015	Importing of GRD products was modified to convert the ground-range data directly to the slant range geometry considering the temporally interpolated gr(sr) polynomials available in the metadata. SCOMPLEX format for the S1 IWS SLC data is supported (besides FCOMPLEX). SLC_cat_S1_TOPS was added to concatenate S1 IWS SLC data. S1_coreg_overlap was updated (supporting the estimation of the azimuth offset refinement using a spectral diversity method considering double difference interferograms in the burst overlap region) S1_subswath_coreg_overlap was added supporting the estimation of the azimuth offset refinement using a spectral diversity method considering double difference interferograms in the burst sub-swath overlap region S1_coreg_TOPS was added to supporting the S1 IWS co-registration sequence using co-registration refinements based on matching and spectral diversity. S1_poly_overlap was added supporting the calculation of polygons for the IWS burst overlap regions S1_deramp_TOPS_reference was added to deramp a S1 IWS reference. S1_deramp_TOPS_slave was added to deramp a S1 IWS co-registered slave. Using OPOD state vectors is supported using the program S1_OPOD_vec

1. Introduction

In this document the support provided in the GAMMA Software for the processing of Sentinel-1 (S1) data is summarized. In particular the use of S1 TOPS mode [3] SLC data for interferometric processing is described in detail as this is significantly different from interferometric processing using strip map mode data.

The basic approach followed is that S1 TOPS mode burst SLC can be imported (→ burst SLC data file and related parameter files). The burst SLC can be detected and mosaiced to get a "mosaic MLI" that includes multiple bursts (along track) and multiple sub-swaths (cross.-track). Similarly, a "mosaic SLC" can be generated – which has the advantage that much of the existing functionality throughout the GAMMA Software can readily be used. To be able to use this approach it is important that the burst SLC geometry is using consistent geometric parameters (including the sampling in slant range and azimuth) between the bursts and between sub-swaths. This aspect was carefully checked and the data was found to meet this requirement.

What is supported with a newly implemented program specifically adapted to the TOPS characteristics is a program for the resampling of a burst SLC to the geometry of a reference burst SLC. In the preparation of the reference and slave burst SLC the programs to concatenate burst SLCs and to copy out a set of indicated bursts from a burst SLC are used to assure that the corresponding bursts are included for the master and the slave.

In addition, a program to extract a single burst of a burst SLC and to write it out as a standard SLC with the corresponding SLC parameter file was implemented as a tool for testing and to provide additional flexibility, e.g. to investigate data in the overlap regions between bursts and sub-swaths.

Furthermore, new programs to deramp SLC and burst SLC data for the azimuth phase ramp related to the variation of the Doppler Centroid were included.

Finally, some typical processing sequences and tests conducted are described. For this we used real Sentinel-1A TOPS mode data that we had available from ESA. To do interferometry with S1 TOPS mode data extremely high co-registration requirements have to be met [4]. In azimuth direction a co-registration accuracy of 0.001 SLC pixel is required to reduce the phase jumps at the burst interface to 3 deg. [4]. Such accuracies can be achieved by considering the double difference phase of the burst overlap areas [5].

The new functionality described is found in the ISP and DIFF&GEO modules.

2. S1 stripmap-mode

2.1. Data import

Sentinel-1 stripmap mode data is imported using the same programs as used for the TOPS data import:

- par_S1_SLC is used to import SLC data
- par_S1_GRD is used to import GRD (detected data in ground-range geometry)

Apart from the GEOTIFF data file xml files containing metadata, calibration information, and noise information are indicated. As output the program generates the SLC or GRD file the corresponding parameter file.

In the metadata the ground-range geometry is characterized with polynomials expressing the ground-range as a function of the slant range (as well as polynomials expressing the slant range as a function of the ground-range). In azimuth direction multiple such polynomials are available. According to the documentation linear interpolation (in time) can be used to get the polynomial for a time between two polynomials. In the ground-range format used in the GAMMA software it is only foreseen to include 3 such polynomials (for the start, center and end time). In the GRD production more polynomials are used and the polynomials are updated over time also considering topographic height information. In order not to degrade the geometry we decided therefore to directly convert the ground-range products to slant range geometry when importing it.

The quality of the imported multi-look intensity (MLI) data files generated from GRD products was checked against SLC data based MLI products and found to be corresponding to mm scale – which is clearly not the case when directly using the imported ground-range products without applying the transformation polynomials.

2.2. Radiometric calibration

In the reading of the SLC and GRD data the radiometric calibration procedure is applied, so that the imported values correspond to backscattering intensities (also for the GRD data it is intensities and not amplitudes!). For the S1 calibration and noise files are used to apply the procedures as described in S1 reference documents.

2.3. Geocoding

Geocoding of S1 stripmap mode data is as for all other sensors. Concerning the quality of the state vector our experience is as follows:

For SLC data the geocoding is almost perfect even without refinement. The refinement determined is usually very small and applying a constant offset is usually sufficient and therefore preferred over refining with linear or quadratic offset polynomials.

For GRD data the geocoding quality achieved based on the state vectors and DEM is also of high quality. It is strongly recommended to do all further steps after the importing using the MLI image in slant-range geometry generated by *par_S1_GRD* . Working with the imported data in ground-range geometry is not recommended because of the reduced geometric accuracy achieved (only 3 ground-range polynomials are stored in the GRD parameter file).

2.4 Other functionality

After the import the S1 stripmap mode data are in the normal SLC or MLI (or GRD) format used in the GAMMA software, making all functionality of the software available.

3. S1 TOPS-mode raw data processing

So far the GAMMA Software does not include a Sentinel-1 raw data processor.

Before October the data available was SLC or GRD data. Then, quite unexpectedly raw data became available (besides GRD data and very few SLC data). In the meantime it is again more SLC data becoming available.

Once the data distribution strategy becomes clearer we will decide if we will implement a TOPS mode data processor for Sentinel-1 as part of the GAMMA Software.

4. S1 TOPS-mode GRD data processing

4.1. Data import

Sentinel-1 GRD (ground-range) data is detected data that was converted to ground-range azimuth geometry. In the reading the calibration procedure is applied, so that the imported values correspond to backscattering intensities (and not amplitudes).

In the slant-range to ground-range conversion ESA applies polynomials which are provided in the meta data. In the calculation of these polynomials a topography model was considered in addition to the orbit data. Consequently the geometry of the GRD products does not fully correspond to the GRD geometry assumed in the GAMMA Software. Furthermore, offsets between two GRD images depend on the transformation applied, which sometime varies between scenes over the same area.

To avoid problems with the geometry of the GRD products we decided to directly convert the GRD products back to the slant range geometry. The converted data corresponds to a multi-look intensity image. Its geometry is specified in the related MLI parameter file. Optionally, e.g. for testing purposes, the GRD data can also be written out in the GRD geometry.

To read in the Sentinel-1 GRD (ground-range) data the program par_S1_GRD is used:

par_S1_GRD s1a-iw-grd-hh.tiff s1a*hh*.xml calibration-s1a-iw-grd-hh-*.xml noise-s1a-iw-grd-hh-*.xml 20140502.hh.mli.par 20140502.hh.mli*

Apart from the GEOTIFF data file xml files containing metadata, calibration information, and noise information are indicated. As output the program generates the MLI file *20140502.hh.mli* and the corresponding parameter file *20140502.hh.mli.par*. **The GRD product is directly converted to the slant range geometry.** Furthermore radiometric calibration is applied.

The geometry of the MLI image was tested against the geometry of an MLI image generated from the corresponding SLC product. The geometries were found to be identical at dm scale. An important advantage of this transformation is that the GRD data can be geocoded at high precision and they can be used well for offset tracking.

An example of an MLI file based on dual pol. TOPS GRD data is shown in Figure 1.

4.2. Radiometric calibration

In the reading of the GRD data the radiometric calibration procedure is applied (respectively the GRD product is already calibrated considering both the calibration and noise data), so that the imported MLI values correspond to backscattering intensities (sigma-zero values using the ellipsoid area as reference area) in slant range geometry.

4.3. Geocoding

To geocoded Sentinel-1 GRD products it is highly recommended to use the imported multi-look intensity image in slant range geometry (and not the ground-range product that can also be generated). The geocoding is done using the program gc_map (and not gc_map_grd which would be for data in ground-range geometry).

For GRD data products the geocoding quality achieved based on the state vectors and DEM is of the same high quality as for the SLC products. Note that typically meter scale quality is achieved even without refinement of the geocoding lookup table.

4.4. Offset tracking

TOPS mode S1 GRD products can be used for offset tracking (program *offset_pwr_trackingm*) to map displacements. For this it is highly recommended to use the imported multi-look intensity image in slant range geometry (and not the ground-range product that can also be generated which may result in anomalies in the offset field). In order to apply a co-registration of the data considering the terrain topography before the determination of the offsets it is recommended to use the co-registration procedure using *rdc_trans*. Furthermore, supportive programs e.g. to calculate the look vector direction or to convert the LOS displacement component to other components are available for the MLI in slant range geometry.

As compared to offset tracking with SLC data a reduced quality is expected for the range offsets because of the multi-looking applied in the generation of the GRD products. Nevertheless, this may be acceptable as the quality of the range offsets will still be higher than the quality of the azimuth offsets.

Considering that the GRD and SLC product based MLI geometries are identical means that it is also possible to do offset tracking between a GRD product and an SLC product.

4.5 Other functionality

After the importing, the GRD data (even if acquired in TOPS mode) is in the normal MLI slant range geometry and format used in the GAMMA software, making all functionality of the software available (e.g. multi-temporal analysis or terrain correction of backscattering coefficients using the *pixel_area* approach).

4.6 Sentinel-1 Extended Wide-Swath (EWS) GRD products

The functionality for Sentinel-1 GRD products is also applicable for the Sentinel-1 Extended Wide-Swath (EWS) GRD products. An example of a geocoded S1 EWS offset field over Svalbard is shown in Figure 2. The result confirms that EWS GRD products can be used for offset tracking, nevertheless the quality of the results is lower than for IWS data because of the lower spatial resolution.

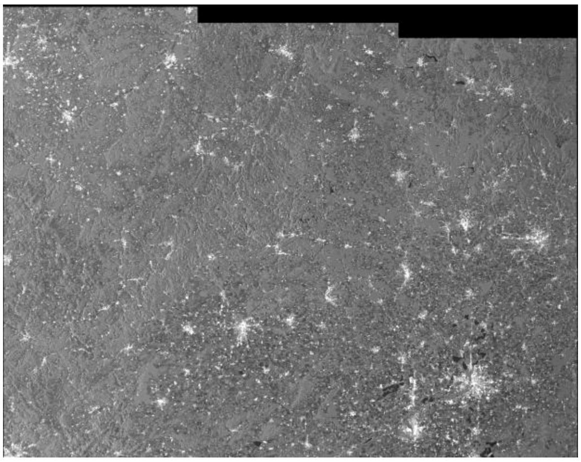

S1-TOPS GRD HH-pol. image 20140502 over Jena, Germany

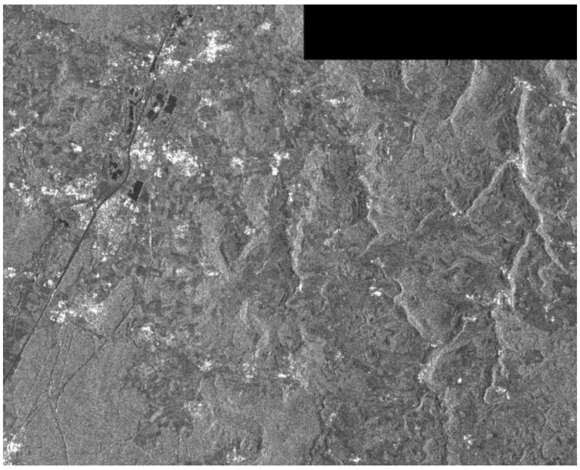

Small section of S1-TOPS GRD HH-pol. image 20140502 over Jena, Germany

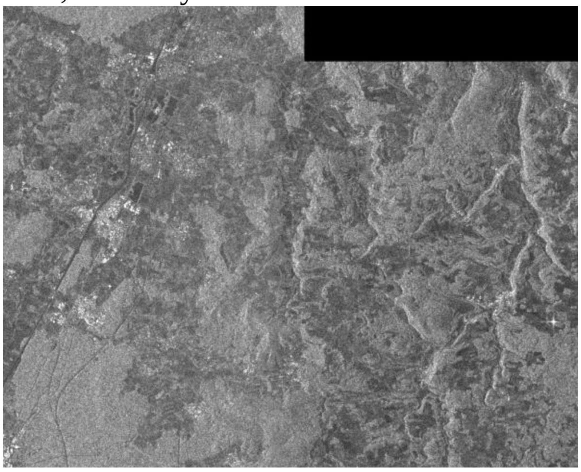

Small section of S1-TOPS GRD HV-pol. image 20140502 over Jena, Germany

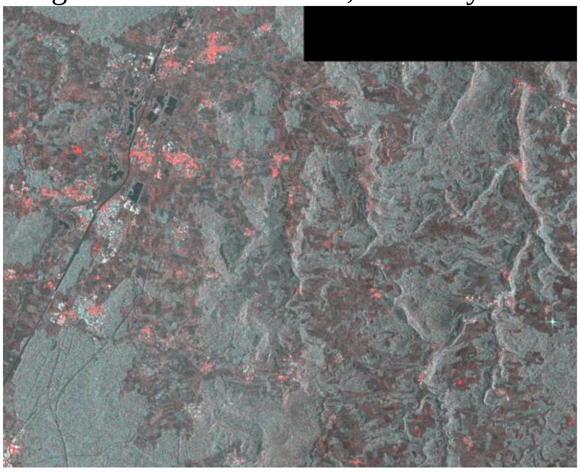

Small section of RGB composite of HH-pol (red) HV-pol (green and blue) HV-pol. image 20140502 over Jena, Germany

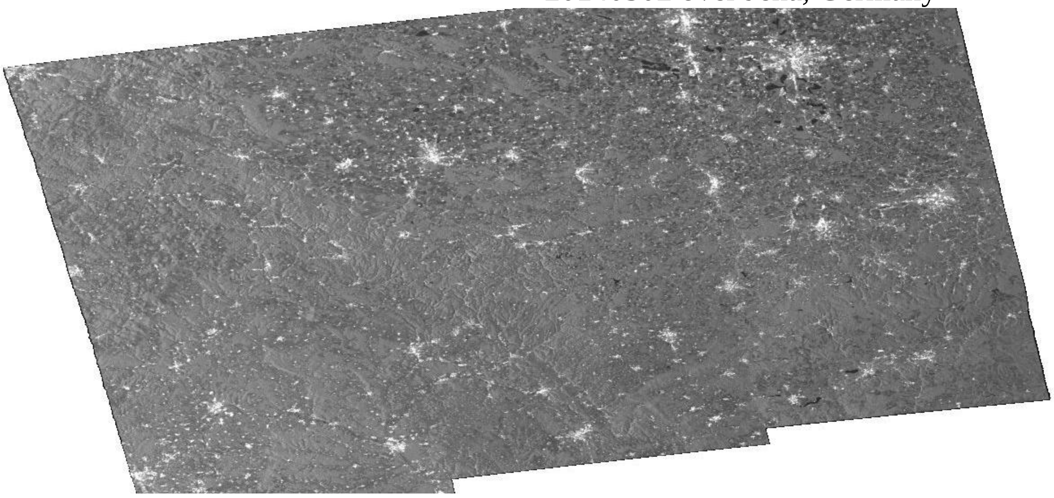

S1-TOPS GRD HH-pol. image 20140502 over Jena, Germany, geocoded to geographic coordinates).

Figure 1 Images derived from dual-pol. S1-TOPS GRD image, 20140502 over Jena, Germany

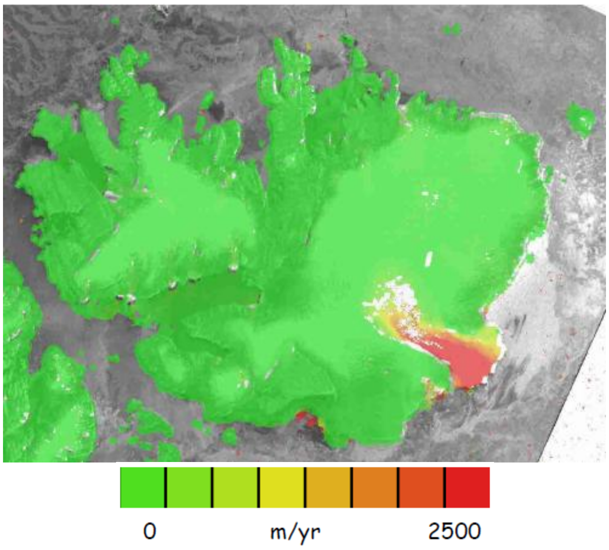

Sentinel-1 IW SLC, 12-day intervals (19/31.01.2015, 20.01/01.02.2015), offset tracking result.

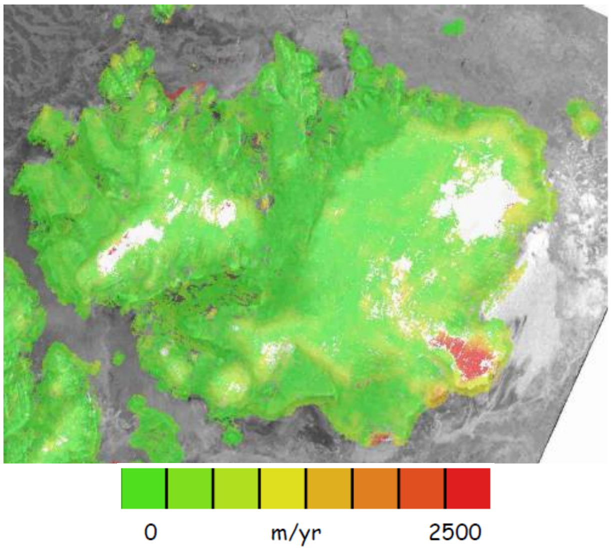

Svalbard. Sentinel-1 EW GRDM, 40 m ground-resolution, 12-day interval (19/31.03.2015), offset tracking result.

Figure 2 Comparison of offset tracking results using a pair of Sentinel-1 IWS SLC Images (left) and a pair of Sentinel-1 EW GRDM data over Svalbard.

5. S1 TOPS-mode SLC data processing

5.1. Data import

S1 TOPS SLC data is typically available as a zip file such as:

S1A_IW_SLC__1SDV_20141003T150845_20141003T150913_002667_002F87_B985.zip

Unzipping this file

unzip S1A_IW_SLC__1SDV_20141003T150845_20141003T150913_002667_002F87_B985.zip

extracts the various data and metadata files into a new directory.

The S1 TOPS SLC data provided by ESA consist of several files out of which we are using:

- the data file (TIFF file)
- the meta data file (XML file) containing information on data, processing, state vectors
- the calibration file (XML file) containing calibration information
- the noise file (XML file) containing information on system noise

For TOPS mode SLC data separate files are provided for each sub-swath.

To read the SLC data and generate the corresponding SLC parameter file the ISP program par_S1_SLC is used:

*par_S1_SLC */*/s1a-iw1-slc-vv-20141003*-004.tiff */*/s1a-iw1-slc-vv-20141003*-004.xml */*/*/calibration-s1a-iw1-slc-vv-20141003*-004.xml */*/*/noise-s1a-iw1-slc-vv-20141003*-004.xml 20141003.IW1.slc.par 20141003.IW1.slc 20141003.IW1.slc.TOPS_par*

which provides 3 output files:

20141003.IW1.slc.par	the „burst SLC parameter file“
20141003.IW1.slc	the „burst SLC file“
20141003.IW1.slc.TOPS_par	the „TOPS parameter file“

The SLC generated is in FCOMPLEX (pair of float) format. Displaying the SLC (here first 1000 lines) can be done using

disSLC 20140502.iw1.hh.slc 20612 1 1000 1. .35 0

In case of TOPS data the SLC data file consists of multiple bursts. A quicklook of the entire sub-swath 1 TOPS SLC data is generate using

rasSLC 20140502.iw1.hh.slc 20612 1 16270 50 10 1. .35 1 0 0 20140502.iw1.hh.slc.ras

and is shown in Figure 3. The bursts are separated by no-data bands. The bursts slightly overlap in along-track or azimuth direction. The data also overlaps between adjacent sub-swaths with a azimuth shift between bursts (see Fig. 4)

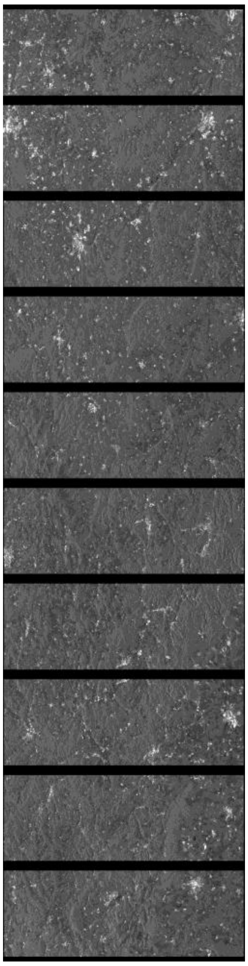

Fig.3 IW1 SLC bursts

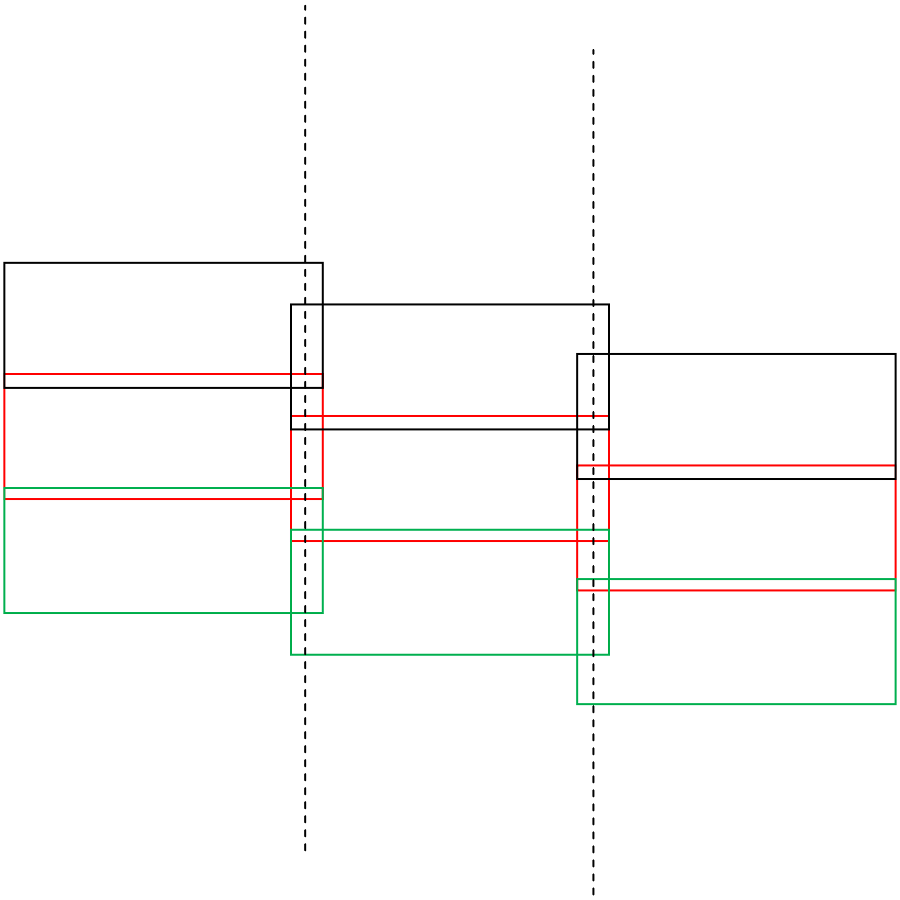

Figure 4 S1 burst structure with small overlaps between bursts and sub-swaths.

For each TOPS mode burst the Doppler Centroid runs through a relatively steep spectral ramp between the beginning and the end of each burst. This can be checked using the program dismph_fft

dismph_fft 20140502.iw1.hh.slc 20612 1 4000 1. .35 32 4 0

Notice that the spectra wrap around several times in the azimuth direction within each burst.

5.2. Radiometric calibration

When reading in the S1 TOPS burst SLC data radiometric calibration is applied using the calibration and noise information from the meta data files available with the data. No special adjustments of the radiometry are done (e.g. based on the overlap regions). Ideally, there should not be any radiometric discontinuities between subsequent bursts or adjacent sub-swaths.

A comparison of the calibrated MLI generated from an IWS SLC product with the MLI generated from the corresponding GRD product is shown in Figure 5. average offset between the two is around -0.1 dB with no trends in range or azimuth and not steps between bursts or sub-swaths visible. Between sub-swaths 2 and 3 a step in the radiometry is visible in both the GRD and SLC based MLIs. This step is better visible in the SLC based MLI, most likely because of the clear cutting between the data coming from one sub-swath and another sub-swath, while averaging of data from both sub-swaths may have been applied for the GRD product (which distributes the step in range direction in the overlap region).

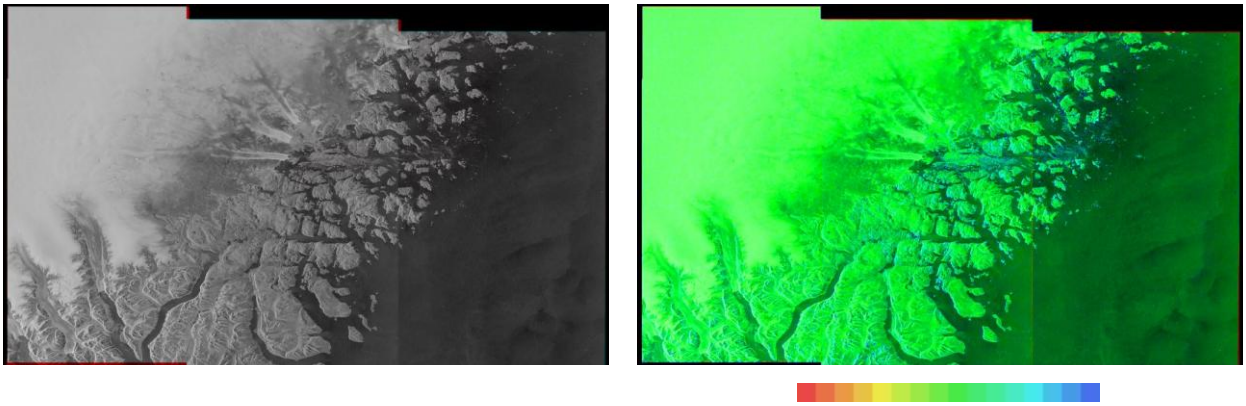

Figure 5 Comparison of radiometry of a calibrated IWS SLC based MLI with the radiometry of the corresponding GRD product based calibrated MLI. The image to the left shows an RGB composite of the GRD based MLI (red channel) and the SLC based MLI (green and blue channels) using the same logarithmic scaling. The image to the right shows the ratio between the two using a logarithmic scaling between -1 dB and +1dB. The

5.3. Concatenate consecutive burst SLCs

The program *SLC_cat_S1_TOPS* concatenates two consecutive burst SLCs into one larger burst SLC. It is a pre-requisite that the bursts of the two input burst SLC match in sequence (no overlap, no gap):

SLC_cat_S1_TOPS SLC_tab1 SLC_tab2 SLC_tab3

SLC_tab1 and SLC_tab2 contain the 3 column lists (SLC SLC_par TOPS_par) for the two input burst SLCs, SLC_tab3 the corresponding names for the output concatenated burst SLC.

Concatenating burst SLCs results in large data files. In order to overcome possible problems with too demanding memory requirements several programs were modified to read only a part of the data into the memory. Furthermore, working with SLC data in SCOMPLEX data is now supported.

5.4. Extract selected bursts into a new burst SLC

The program *SLC_copy_S1_TOPS* extracts an indicated selection of bursts from a burst SLC:

SLC_copy_S1_TOPS 20150323.SLC_tab.tmp 20150323.SLC_tab 1 1 3 8

extracts all the bursts between the first burst of IW1 and burst 8 of IW3 resulting in an output burst SLC with 8 bursts in all 3 sub-swaths. This functionality can be used to reduce the data set to the area of interest and to assure that an interferometric pair includes the same bursts. To reduce the burst SLC to only two or one sub-swath is easily possible by adjusting the input SLC table accordingly (e.g. only one line for IW3 to only include IW3).

5.5. Extract data of single bursts into a standard SLC

The program *SLC_burst_copy* supports the extraction of a single burst of a TOPS SLC into a standard SLC file with the corresponding SLC parameter file. To extract the third burst of the first sub-swath use

SLC_burst_copy 20140502.iw1.hh.slc 20140502.iw1.hh.slc.par 20140502.iw1.hh.TOPS_par 20140502.iw1.hh.burst3.slc 20140502.iw1.hh.burst3.slc.par 3 1 1.

This functionality is for example suited to check the data in overlap regions between bursts. An example of an investigation in an overlap region is shown in Figure 8.

In our development we used this functionality to check the geometric consistency between subsequent bursts and between adjacent sub-swaths.

5.6. MLI mosaic

Detection of TOPS burst SLC data, multi-looking, and mosaicing of TOPS burst SLC data from multiple bursts and multiple sub-swaths into one (standard) output MLI with a MLI parameter file that contains the geometric information for the MLI is supported by the program *multi_S1_TOPS*.

A first relevant aspect the program solves is to decide which data of which burst is used. The normal strategy is that even in overlap regions (between bursts or sub-swaths) only data from one burst is used. As a result a more homogeneous radiometric quality is achieved (no spatial jumps in equivalent number of looks). In the determination of where the cut between two bursts shall be the multi-looking is considered such that multi-looking is only done between pixels originating from the same burst and same sub-swath.

The data to be considered is listed in an ascii file here called SLC_tab (3 column list of SLC, SLC_par, TOPS_par sorted from near to far range) such as

20140502.iw1.hh.slc 20140502.iw1.hh.slc.par 20140502.iw1.hh.TOPS_par
20140502.iw2.hh.slc 20140502.iw2.hh.slc.par 20140502.iw2.hh.TOPS_par
20140502.iw3.hh.slc 20140502.iw3.hh.slc.par 20140502.iw3.hh.TOPS_par

Then the program *multi_S1_TOPS* is used to do the detection, multi-looking, and mosaicing into a single output geometry

multi_S1_TOPS SLC_tab 20140502.mli 20140502.mli.par 10 2

The output MLI is shown in Figure 6. Figure 7 shows as section that includes transitions in both along track (between bursts) and slant range (between sub-swaths) at high resolution (5 range looks x 1 azimuth look). As you can see the geometric and radiometric correspondence is very good without application of any kind of geometric or radiometric refinement.

The spatial resolution of the TOPS SLC data is such that a stronger multi-looking in range than in azimuth is recommended (which is different from what we are used to for ERS or ENVISAT). This can be for example 5 looks in range and 1 look in azimuth (or multiples thereof). At full resolution MLI image files can get very large.

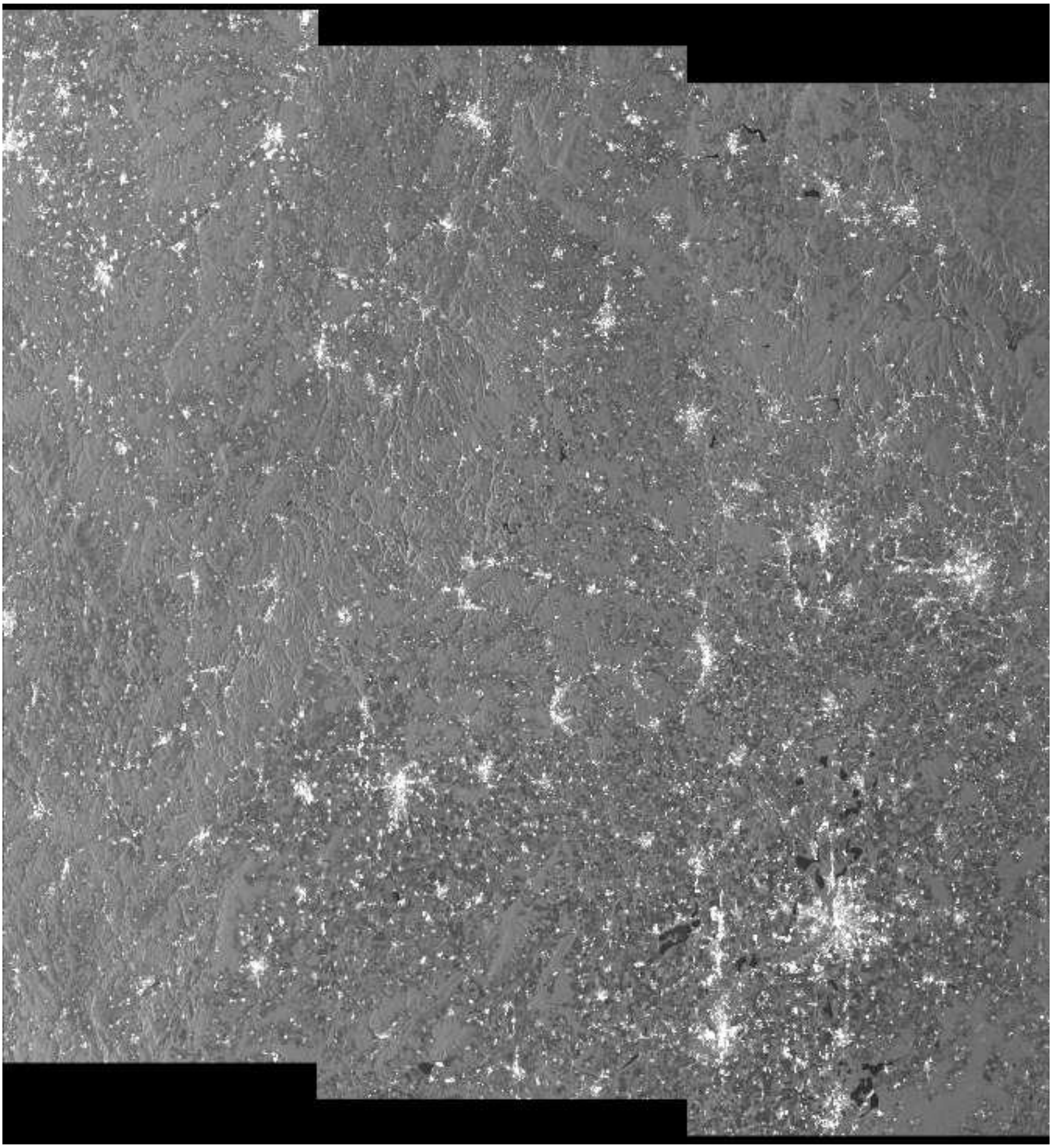

Figure 6 MLI mosaic for a “full Sentinel-1 TOPS scene” consisting of 3 sub-swaths with 10 bursts each.

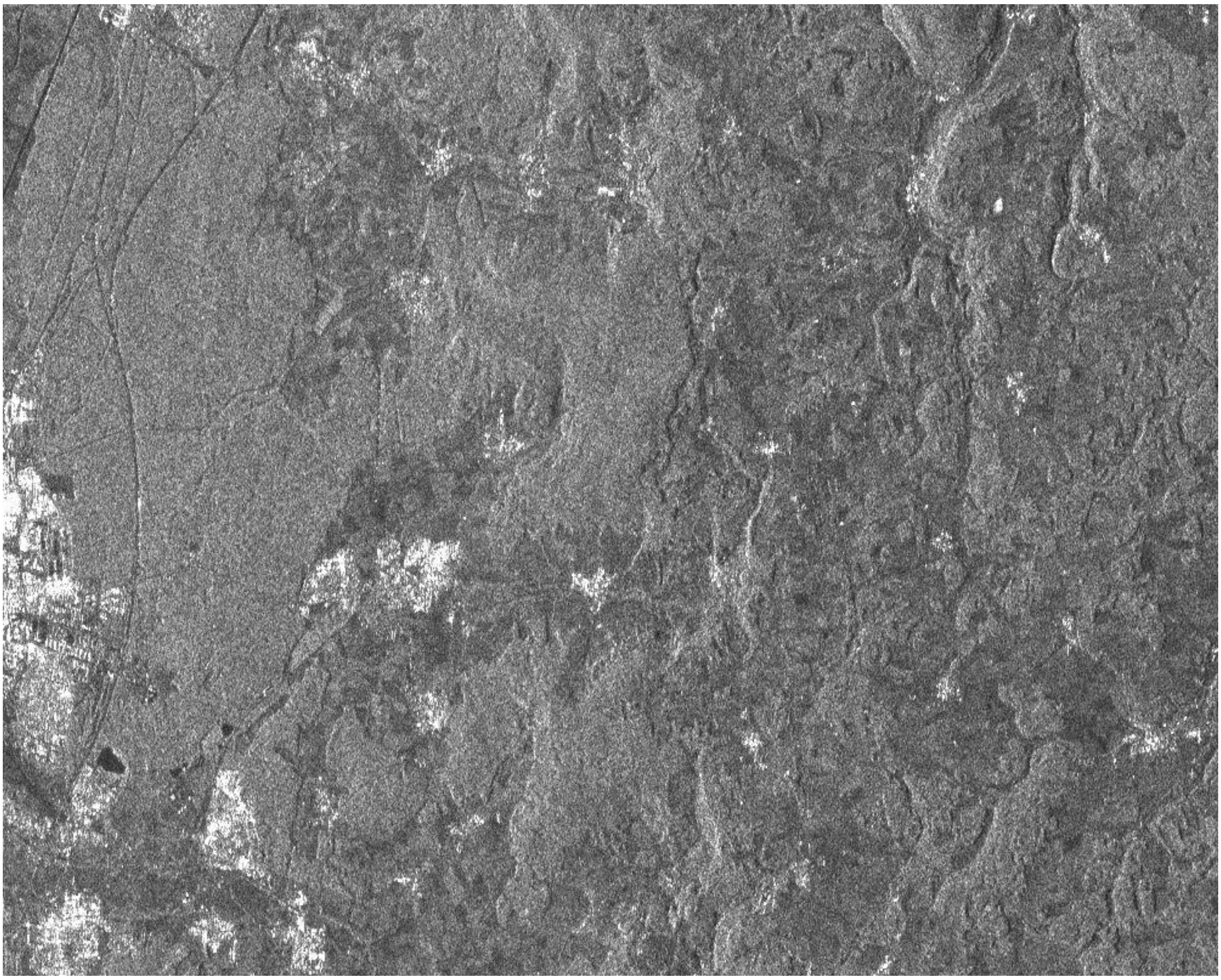

Figure 7 Transitions section (between bursts and between sub-swaths) in MLI mosaic shown at high resolution (5 range looks x 1 azimuth look). The transition between the bursts and sub-swaths is exactly in the centers of the image. As you can see the geometric and radiometric correspondence is very good without application of any kind of geometric or radiometric refinement.

5.7. SLC mosaic

It is also possible to generate an SLC mosaic for a S1 TOPS SLC data set. It has to be kept in mind though, that the Doppler Centroid will strongly vary within the mosaic with strong steps at the interface between subsequent bursts. When further using the mosaic SLC, e.g. for interferometry, it is relevant that only data originating from corresponding bursts are interferometrically combined; therefore we anticipate in the SLC mosaic generation what multi-looking will be used later on and connect the bursts accordingly. For this reason it is necessary to indicate the range and azimuth looks that will be used later on. The SLC mosaic is generated using the program SLC_mosaic_S1_TOPS

SLC_mosaic_S1_TOPS SLC1_tab 20141003.slc 20141003.slc.par 10 2

The mosaic SLC of an entire S1 TOPS scene (e.g. with 9 bursts) gets quite large with around 68000 range samples and about 13000 azimuth lines (in FCOMPLEX format), which results in filesizes > 7 GByte in FCOMPLEX and 3.5 GByte in SCOMPLEX format.

In principle the mosaic SLC with the corresponding SLC parameter file can be used with all the programs for SLC data in the GAMMA Software. Some care is necessary though because of the Doppler Centroid variation within mosaic SLC. In particular interpolators (e.g. used when resampling the data or when oversampling the data) need to consider the spectral properties. Consequently, a specific strategy for the resampling of the TOPS data was implemented (see below) and programs to deramp the azimuth phase ramp from the Doppler Centroid variation are included in the software. (see below).

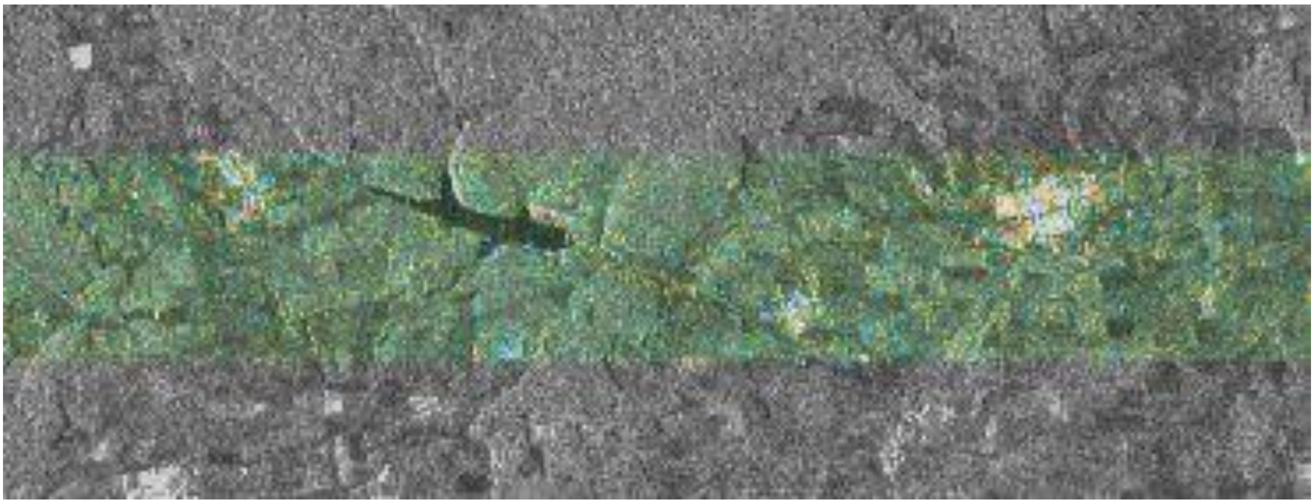

Figure 8 Hue-intensity-saturation composite of the backscatter change in dB between two overlapping bursts, average backscatter of two bursts, and absolute value of backscatter change in dB between two overlapping bursts, shown for an overlap region between two subsequent bursts. The total area shown corresponds to the total burst overlap (including null values). The area with color shows the actual data overlap. Pixels with color correspond to areas with significant backscatter difference between the two bursts, probably relating to directional scattering effects caused by the different Doppler Centroids).

5.8. Azimuth Spectrum Deramping

For each TOPS mode burst the Doppler Centroid runs through a relatively steep spectral ramp between the beginning and the end of each burst. This can be checked using the program dismph_fft

dismph_fft 20140502.iw1.hh.slc 20612 1 4000 1. .35 32 4 0

Notice that the spectra wrap around several times in the azimuth direction within each burst. This phase ramp needs to be considered in some processing steps (e.g. when interpolating SLC data). While some programs were adapted for this others are not or the related spectral information is not available as in the case of the SLC mosaic. For this reason programs to deramp SLC data for this azimuth spectrum ramp are included in the software for burst SLC data (program *SLC_deramp_S1_TOPS*) as well as for normal SLC data (e.g. data of a single burst → program *SLC_deramp*)

To deramp a burst SLC the following command is used:

SLC_deramp_S1_TOPS SLC1_tab SLC2_tab 0 1

The burst SLC data specified in SLC1_tab is deramped and written out to the burst SLC data as specified in SLC2_tab. Besides, the deramped burst SLC for the different sub-swaths the program also writes out the phase ramp (float format file) that was subtracted (file names are generated by adding .dph to the burst SLC filenames).

To deramp a normal SLC the following command is used:

SLC_deramp 20140502.iw1.burst1.hh.slc 20140502.iw1.burst1.hh.slc.par 20140502.iw1.burst1.hh.slc.deramp 20140502.iw1.burst1.hh.slc.deramp.par 0

The deramped SLC can be displayed using the program *dismph_fft* to check that the azimuth spectrum changed in the expected manner.

To deramp a TOPS SLC mosaic it is necessary to deramp the individual burst SLCs for all the sub-swaths before generating the mosaic.

Notice that deramping means the subtraction of a phase ramp. Consequently, it influences interferometry (as the phases are changed).

5.9. Geocoding

Geocoding of TOPS data (when starting from burst SLC files) is done by first generating a MLI mosaic. This is either done by generating an SLC mosaic using *SLC_mosaic_S1_TOPS* followed by multi-look and detection using *multi_look,* or it is done directly using the MLI mosaic program *multi_S1_TOPS*.

Geocoding is then done for the mosaic MLI as for a normal MLI. For the geocoding of S1 data the method with *gc_map* that also considers the effects of the ellipsoid and the terrain heights is used. In the following a possible geocoding sequence is indicated (starting from the burst SLC data.

S1 TOPS data geocoding (starting from burst SLC)

1) Generate SLC_tab for the burst SLC (including all 3 sub-subswaths)

echo 20141003.IW1.slc 20141003.IW1.slc.par 20141003.IW1.slc.TOPS_par" > SLC1_tab

echo 20141003.IW2.slc 20141003.IW2.slc.par 20141003.IW2.slc.TOPS_par" >> SLC1_tab

20141003.IW3.slc 20141003.IW3.slc.par 20141003.IW3.slc.TOPS_par" >> SLC1_tab

2) Generate SLC mosaic

SLC_mosaic_S1_TOPS SLC1_tab 20141003.slc 20141003.slc.par 10 2

3) Multi-looking and detection

multi_look 20141003.slc 20141003.slc.par 20141003.slc.mli 20141003.slc.mli.par 10 2

10 range and 2 azimuth looks are used in this example. The resulting MLI can be displayed e.g. using dispwr (see Figure 9)

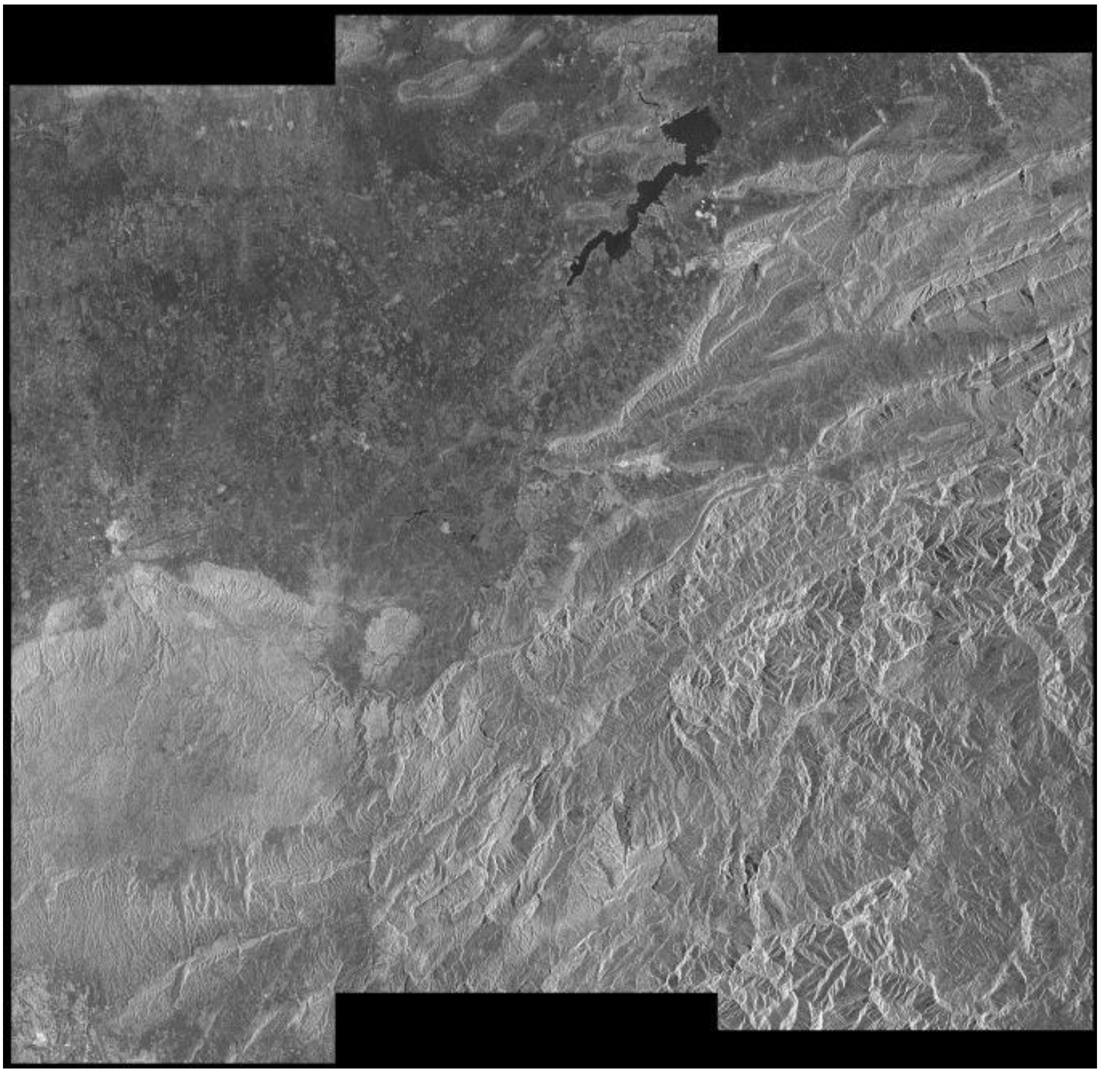

Figure 9 MLI mosaic 20141003.slc.mli that includes 3 sub-swaths. Data is over Iraq, acquired from an ascending orbit, and shown in slant range and azimuth geometry.

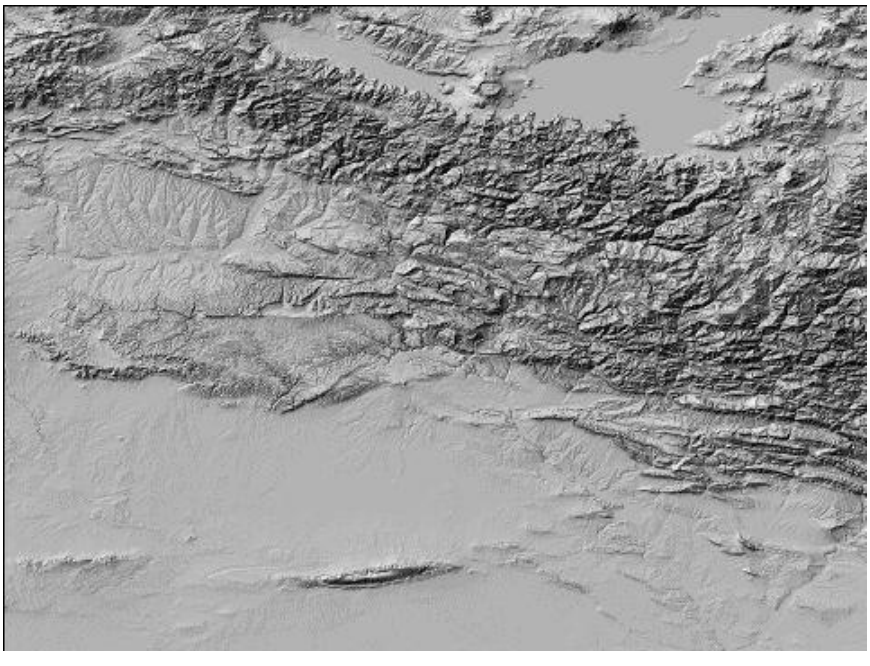

Figure 10 SRTM DEM section used.

4) Preparation of DEM that covers at least the area of interest

For the example we prepared the SRTM heights (assuring that the heights are WGS84 heights and not heights above the geoid, Figure 10).

5) Derive geocoding lookup table

The geocoding lookup table is generated using *gc_map*

gc_map 20141003.slc.mli.par - SRTM.dem_par SRTM.dem EQA.dem_par EQA.dem 20141003.lt 4 5 20141003.sim_sar u v inc psi pix ls_map 8 2

The input DEM, SRTM.dem with SRTM.dem_par, is oversampled with a factor 4 in longitude and a factor 5 in latitude to result in pixels of about 20m in both dimensions.

6) Refinement of geocoding lookup table using procedure with pixel_area

For the refinement of the geocoding lookup table we describe here the procedure that uses the program pixel_area to calculate a simulated backscatter image based on the DEM. This simulated image, pix_gamma0, is in the slant range geometry:

pixel_area 20141003.slc.mli.par EQA.dem_par EQA.dem 20141003.lt ls_map inc pix_sigma0 pix_gamma0

Using dis2pwr can be used to visualize the simulated image and the MLI image

dis2pwr pix_gamma0 20141003.slc.mli 6819 6819

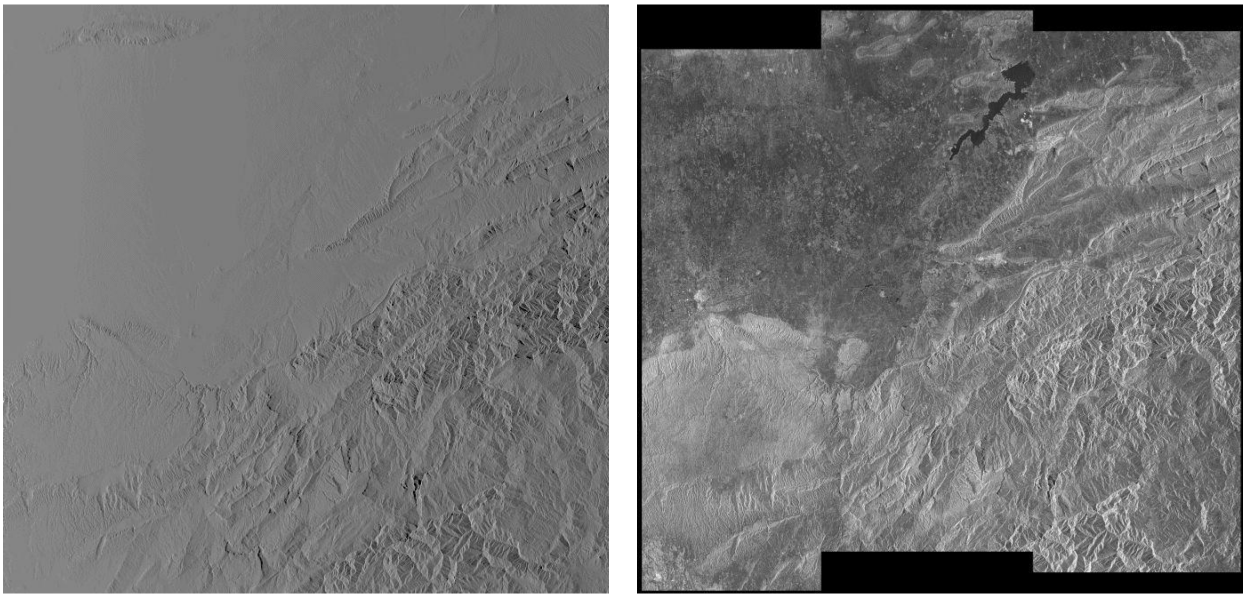

Figure 11 Simulated (left) and real MLI image (right) used to determine geocoding lookup table refinement.

Based on the simulated and real MLI images (Figure 11) a correction to the geocoding lookup table is determined and applied:

create_diff_par 20141003.slc.mli.par - 20141003.diff_par 1 0

offset_pwrm pix_sigma0 20141003.slc.mli 20141003.diff_par 20141003.offs 20141003.snr 256 256 offsets 2 64 64 7.0

offset_fitm 20141003.offs 20141003.snr 20141003.diff_par coffs coffsets 7.0 1

gc_map_fine 20141003.lt 19200 20141003.diff_par 20141003.lt_fine 1

Here only a constant offset is used in the refinement polynomial determined with offset_fitm. It seems a higher order correction (linear or quadratic polynomials) is not necessary given the high quality of the S1 orbit data. The quality of the refinement is documented in the screen output of the program offset_fitm:

final solution: 2045 offset estimates accepted out of 4096 samples
final range offset poly. coeff.: 0.02599
final azimuth offset poly. coeff.: 0.00238
final range offset poly. coeff. errors: 2.26268e-04
final azimuth offset poly. coeff. errors: 1.29664e-04
final model fit std. dev. (samples) range: 0.1876 azimuth: 0.1075

Notice that the determined correction is only a small fraction of an MLI pixel – therefore even without refinement a good geocoding quality is achieved.

8) Use geocoding lookup table to geocode MLI image

Geocoding from SAR to map geometry is then done using *geocode_back*

geocode_back 20141003.slc.mli 6819 20141003.lt_fine EQA.20141003.slc.mli 19226 9860 2 0

The geocoded backscatter image is shown in Figure 12.

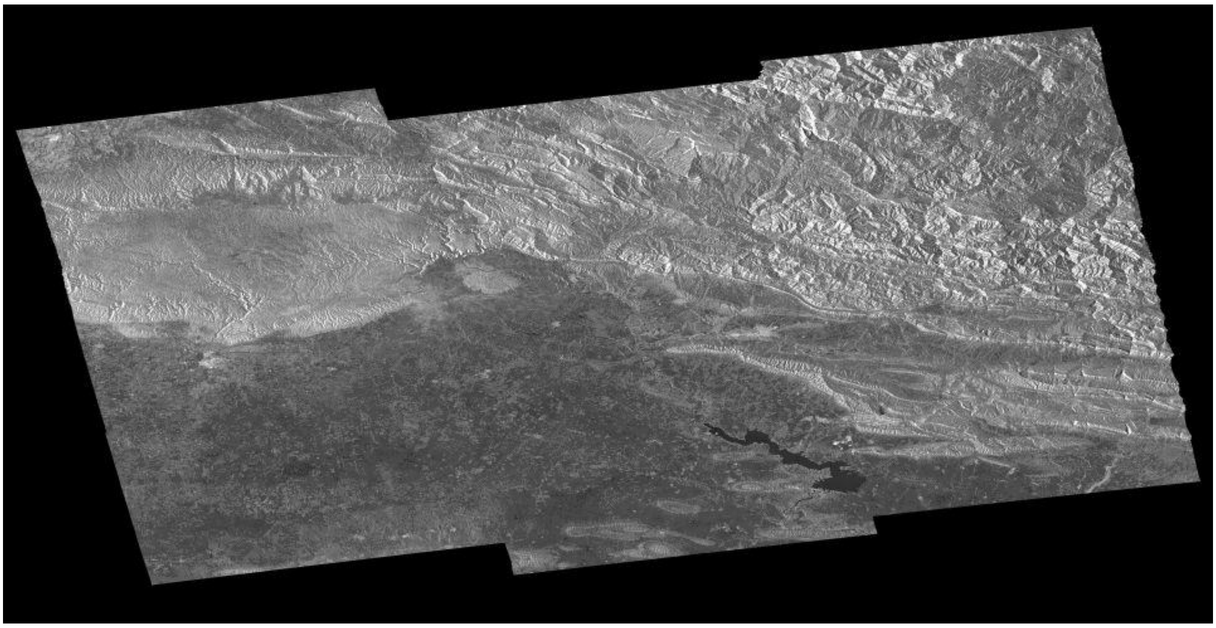

Figure 12 S1 TOPS geocoded backscatter image.

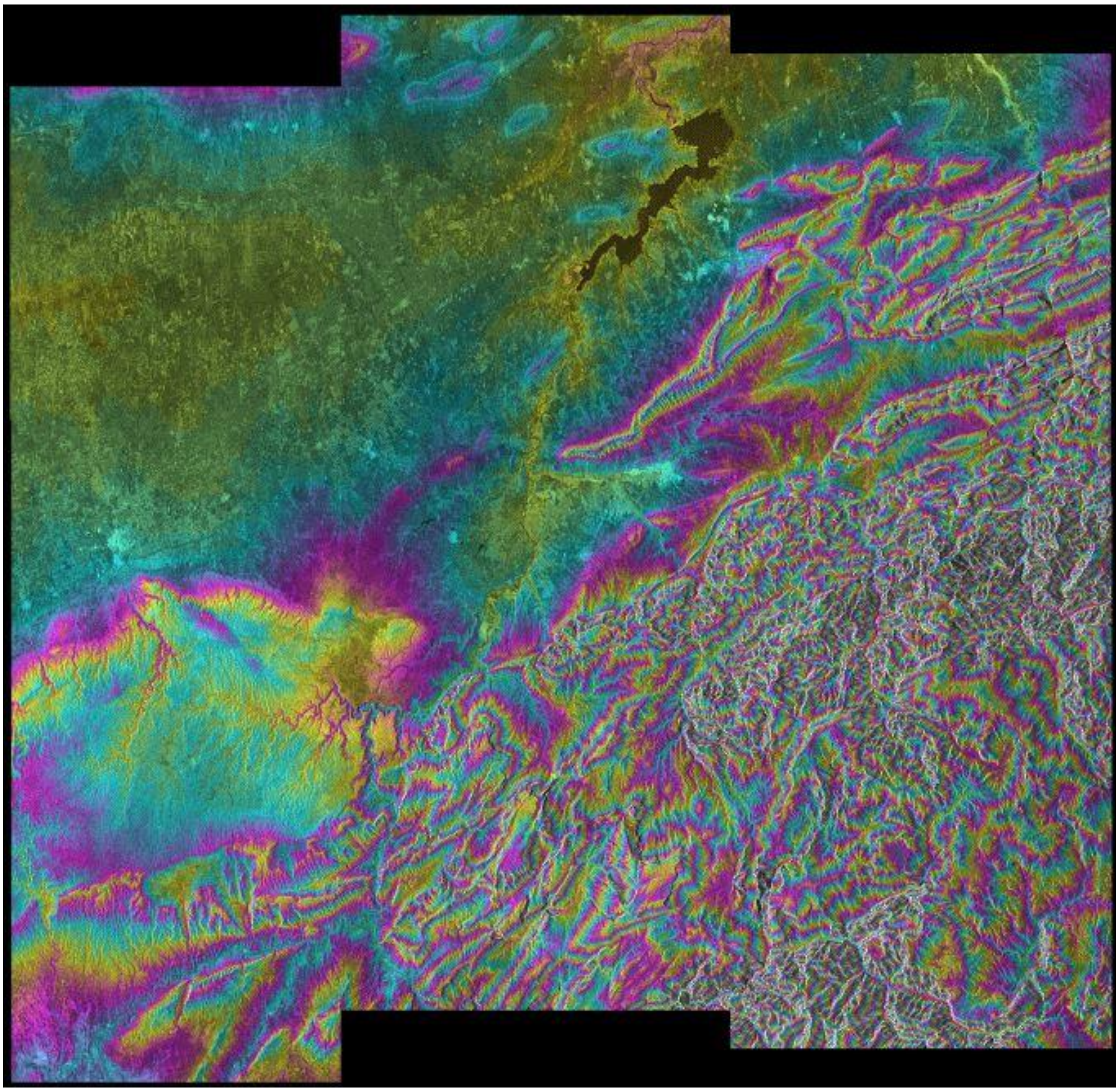

Figure 13 DEM heights superposed to the backscatter intensity (in SAR geometry of the MLI). The heights are shown using a cyclic color scale with 500m per color cycle.

9) Use geocoding lookup table to transform DEM heights into SAR geometry (of the MLI)

The transformation of the DEM heights into SAR geometry of the MLI is done using *geocoded*:

geocode 20141003.lt_fine EQA.dem 19226 20141003.hgt 6819 6634 2 0

The file 20141003.hgt is shown in Figure 13.

Observation:

The geocoding is almost perfect even without refinement. The refinement determined is usually very small and applying a constant offset is usually sufficient and therefore preferred over refining with linear or quadratic offset polynomials.

5.10 Other functionality

Most of the functionality of the GAMMA Software is applicable to the S1 TOPS data – e.g. using the mosaic SLC and MLI. For the special case of interferometry (including an extensive section on S1 TOPS SLC co-registration) and for PSI this is further discussed below.

6. S1 TOPS-mode Interferometry

In this section the processing of an S1 TOPS interferogram is described in detail. Besides the main sequence some options (e.g. to further iterate certain steps) are described. The larger part of the processing is reserved for the TOPS burst SLC co-registration (Section 6.1). Here an extremely accurate co-registration in the azimuth direction is required and therefore the refinement of the co-registration is done very carefully, using several methods and potentially iterating some of the steps to maximize the quality achieved. The interferogram generation as such (Section 6.2) is then as for standard SLCs. An important aspect of the discussion is also the quality control for the individual steps.

As presented the procedure is not optimized for processing speed but rather to achieve a good robustness of the processing. In section 6.1 the co-registration procedure is described step by step. Then, in section 6.2, the same process supported by a script that automates these steps and that makes the process also more efficient is discussed.

6.1. TOPS SLC co-registration

The processing strategy used for the co-registration of a pair of S1 TOPS SLC is very important because interferometry with S1 TOPS data requires an extremely precise co-registration of the SLC pairs. In the azimuth direction an accuracy of a few thousand’s of a pixel is absolutely required, otherwise phase jumps between subsequent bursts are observed.

To assure this very high co-registration accuracy the method that considers the topography has to be used (using *rdc_trans*). To determine the refinement of the transformation lookup table calculated using *rdc_trans* (i.e. based on the orbit and DEM data) we can use several methods. Furthermore, the results need to be tested (e.g. by calculating the differential interferogram to check it visually for phase jumps at the interfaces between subsequent bursts).

Normally, more than one method is applied to iteratively improve the co-registration refinement. Typically, this includes first a matching procedure as supported by *offset_pwr* and then a spectral diversity method (as supported by the shell script *S1_coreg_overlap*) that considers the interferometric phase of the burst overlap region.

The refinement determined is only a constant offset in slant range and in azimuth (the same correction is applicable for all bursts and all sub-swaths).

In the following description some "optional steps" are mentioned besides the main steps necessary to process a “typical example”. Such optional steps are shown to indicate possibilities to make the processing successful in cases that may be more difficult e.g. because of lower coherence.

6.1.1) Preparation of S1 IWS reference and slave images

As a preparation step it is recommended to assure that the S1 IWS scene selected as reference and the corresponding slave scene that should be brought into the reference geometry, both include the **identical sub-swaths and bursts**. For pairs where this is not the case for the data obtained this is assured using SLC_cat_S1_TOPS (to concatenate subsequent IWS scenes) and SLC_copy_S1_TOPS (to copy out the corresponding bursts). If this preparation is not done some later steps may fail.

6.1.2) Calculate co-registration lookup table using rdc_trans

Then we calculate the co-registration lookup table between MLI mosaic of the **S1 TOPS SLC master (**20141003.slc.mli) and MLI mosaic of the **S1 TOPS SLC slave**

(20141015.slc.mli). The MLI mosaic is calculated using the program multi_look (with the IWS SLC mosaic as input). The lookup table is calculated using *rdc_trans*, so that the terrain topography (available in 20141003.hgt) is considered.

rdc_trans 20141003.slc.mli.par 20141003.hgt 20141015.slc.mli.par 20141015.slc.mli.lt

the derived lookup table (20141015.slc.mli.lt) permits to resample data between the master and slave geometries.

Optionally, we can refine this lookup table by transformation of the master MLI mosaic into the slave MLI mosaic geometry (using *geocode*). Then we can determine a constant offset between the two using *create_diff_par* to create the *DIFF_par* file, then *offset_pwrm* to determine the offset field, *offset_fitm* to estimate the constant range and azimuth offset, and *gc_map_fine* to update the lookup table for this correction. Considering that the orbit data are very accurate for S1 this refinement is not done – this refinement step is more well suited for the estimation and correction of larger (> 1 pixel) offsets, but not so precise for very small offsets because multi-looked data are used.

The program *SLC_copy_S1_TOPS* can be used to copy a smaller block out of a S1 TOPS burst SLC. This can also be used to assure that both data sets of an interferometric pair include the same sub-swaths and bursts.

6.1.3) Determine refinement using matching techniques

Then we determine a refinement to the co-registration lookup table. For this we determine offsets between the SLC master and the resampled SLC slave (considering the lookup table without refinement). To determine the offset between the SLC master and the resampled SLC slave we have to first resample the the S1 TOPS SLC slave to the master geometry. This is done using the program *SLC_interp_lt_S1_TOPS*. To run it, we have to first generate an SLC_tab (RSLC2_tab) for the output resampled slave burst SLC:

echo "20141015.IW1.rslc 20141015.IW1.rslc.par 20141015.IW1.rslc.TOPS_par" > RSLC2_tab

echo "20141015.IW2.rslc 20141015.IW2.rslc.par 20141015.IW2.rslc.TOPS_par" >> RSLC2_tab

echo "20141015.IW3.rslc 20141015.IW3.rslc.par 20141015.IW3.rslc.TOPS_par" >> RSLC2_tab

we can then resample the S1 TOPS SLC slave. The output is again a burst SLC with separate files for each sub-swath. In this manner the entire bursts are resampled, including the full burst overlap areas

SLC_interp_lt_S1_TOPS SLC2_tab 20141015.slc.par SLC1_tab 20141003.slc.par 20141015.slc.mli.lt_fine 20141003.slc.mli.par 20141015.slc.mli.par - RSLC2_tab 20141015.rslc 20141015.rslc.par

Instead of an offset parameter file a "-" is provided as no refinement is available at this stage. Besides the resampled burst SLC the program SLC_interp_lt_S1_TOPS also writes out a mosaic SLC for the resampled slave SLC (*20141015.rslc 20141015.rslc.par*).

Using *offset_pwr* and *offset_fit* we determine now the residual offset between the master SLC mosaic and the slave SLC mosaic using the RSLC cross-correlation method:

create_offset 20141003.slc.par 20141015.slc.par 20141003_20141015.off 1 10 2 0

offset_pwr 20141003.slc 20141015.rslc 20141003.slc.par 20141015.rslc.par 20141003_20141015.off 20141003_20141015.offs 20141003_20141015.snr 256 64 - 1 64 64 7.0 4 0 0

offset_fit 20141003_20141015.offs 20141003_20141015.snr 20141003_20141015.off - - 10.0 1 0

Notice that <u>we don't apply an SLC oversampling in *offset_pwr*</u> as the procedure used is not ideal because of the strong Doppler Centroid variations (unless the burst SLCs were deramped first). Furthermore, working without oversampling is faster.

In *offset_fit* we only estimate a constant offset in range and azimuth (and no linear or quadratic offset polynomial). Correcting an offset only is sufficient! The screen output of *offset_fit* shows us that the offset estimated is a fraction of an SLC pixel only and it is estimated with a good accuracy (low standard deviation, many estimates):

final solution: 2350 offset estimates accepted out of 4096 samples
final range offset poly. coeff.: -0.05248
final range offset poly. coeff. errors: 1.69248e-05
final azimuth offset poly. coeff.: -0.28359
final azimuth offset poly. coeff. errors: 2.00844e-05
final model fit std. dev. (samples) range: 0.0212 azimuth: 0.0251

Considering that we want to achieve an accuracy of a very small fraction of an SLC pixel, especially in the azimuth direction, we typically iterate this offset estimation. This is done typically once, but at least until the azimuth offset correction becomes smaller than 0.02 SLC pixel.

For this iteration we have to resample again the S1 TOPS SLC slave with *SLC_interp_lt_S1_TOPS*, but this time indicating the offset correction (*20141003_20141015.off*):

SLC_interp_lt_S1_TOPS SLC2_tab 20141015.slc.par SLC1_tab 20141003.slc.par 20141015.slc.mli.lt_fine 20141003.slc.mli.par 20141015.slc.mli.par 20141003_20141015.off RSLC2_tab 20141015.rslc 20141015.rslc.par

Then we define an new offset parameter file and estimate again a residual offset between the master SLC mosaic and the slave SLC mosaic using the RSLC cross-correlation method:

create_offset 20141003.slc.par 20141015.slc.par 20141003_20141015.off1 1 10 2 0

offset_pwr 20141003.slc 20141015.rslc 20141003.slc.par 20141015.rslc.par 20141003_20141015.off1 20141003_20141015.offs 20141003_20141015.snr 256 64 - 1 64 64 7.0 4 0 0

offset_fit 20141003_20141015.offs 20141003_20141015.snr 20141003_20141015.off1 - - 10.0 1 0

This time the residual azimuth offset found is below 0.02 azimuth pixel. Consequently we don’t further iterate the procedure

final solution: 2330 offset estimates accepted out of 4096 samples
final range offset poly. coeff.: -0.01754
final range offset poly. coeff. errors: 1.42203e-05
final azimuth offset poly. coeff.: ***-0.01311*** *(which is < 0.02)*
final azimuth offset poly. coeff. errors: 1.63548e-05
final model fit std. dev. (samples) range: 0.0179 azimuth: 0.0205

We update the offset parameter file to include the total offset estimated (in *20141003_20141015.off.total*)

offset_add 20141003_20141015.off 20141003_20141015.off1 20141003_20141015.off.total

and use the total offset (*20141003_20141015.off.total*) to resample again the S1 TOPS SLC slave with SLC_interp_lt_S1_TOPS

SLC_interp_lt_S1_TOPS SLC2_tab 20141015.slc.par SLC1_tab 20141003.slc.par 20141015.slc.mli.lt_fine 20141003.slc.mli.par 20141015.slc.mli.par 20141003_20141015.off.total RSLC2_tab 20141015.rslc 20141015.rslc.par

At this stage the 2 master and slave burst SLC should already be co-registered at 1/100 azimuth pixel level. For an optional test we can therefore calculate the differential interferogram. We expect to see that there are still phase jumps between the bursts but the phase jumps are expected to be below a full phase cycle. The differential interferogram is calculated using the co-registered master and slave mosaic SLCs using the normal approach of the gamma software (with *phase_sim_orb* and *SLC_diff_intf*):

phase_sim_orb 20141003.slc.par 20141015.slc.par 20141003_20141015.off 20141003.hgt 20141003_20141015.sim_unw 20141003.slc.par - - 1 1

SLC_diff_intf 20141003.slc 20141015.rslc 20141003.slc.par 20141015.rslc.par 20141003_20141015.off 20141003_20141015.sim_unw 20141003_20141015.diff.test1 10 2 0 0 0.2 1 1

The resulting differential interferogram can be visualized for example using *dismph_pwr*. An overview of a possible result is shown in Figure 14. Some phase jumps are clearly visible. For other burst transitions this is not obvious. It is also quite clear that the phase discontinuities are clearly smaller than a full phase cycle.

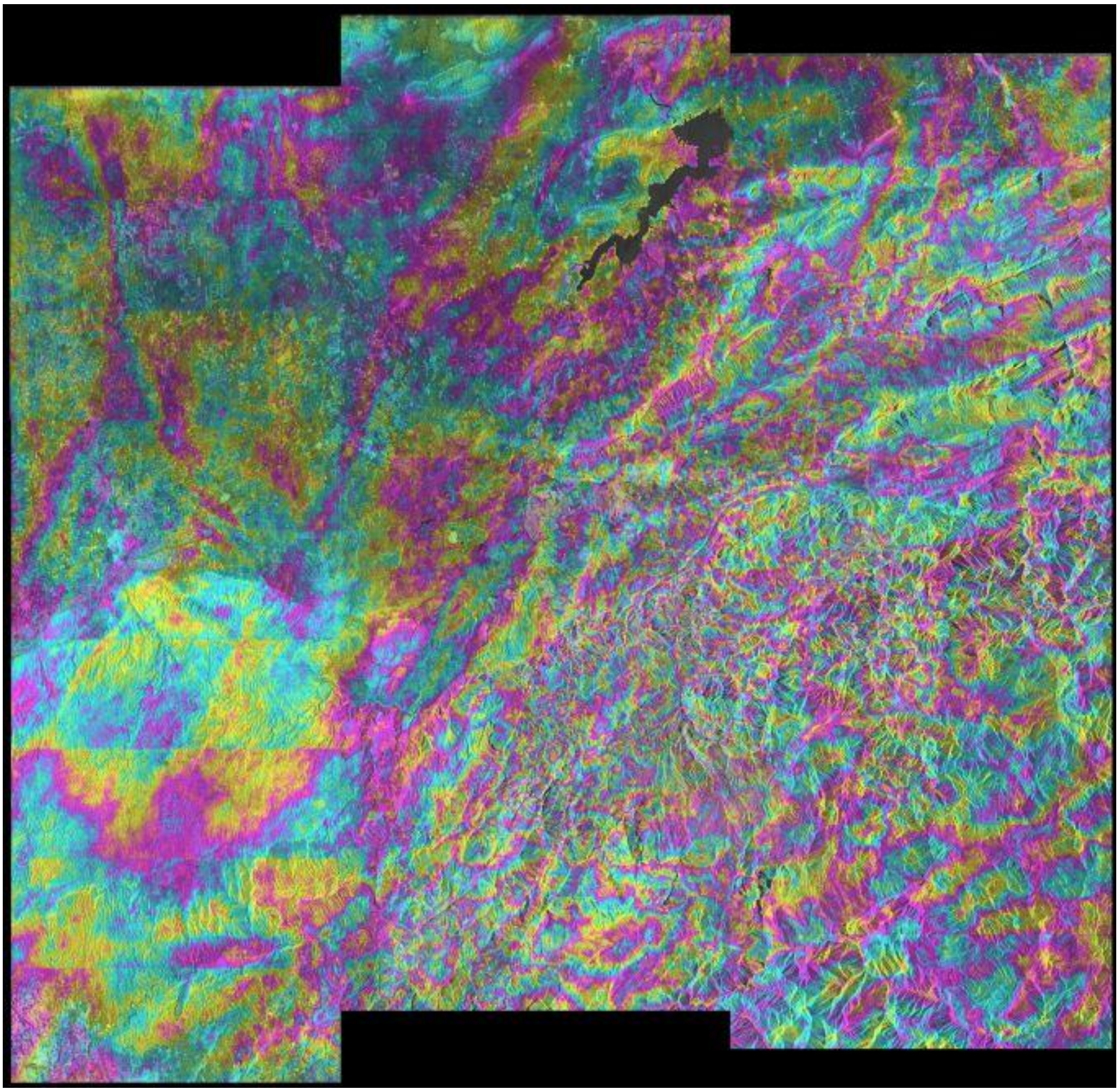

Figure 14 S1 TOPS differential interferogram as obtained using refined co-registration after the refinement using the matching procedure. One color cycle corresponds to one phase cycle.

6.1.4) Determine refinement of the azimuth offset using a spectral diversity method that considers the double difference phase in the burst overlap regions

Then we determine a refinement of the azimuth offset estimation using a spectral diversity method that considers the double difference phase in the burst overlap regions. The strong Doppler variation within each burst results in significant phase effects if the co-registration in azimuth direction is not perfect. This effect is very significant. Even an azimuth mis-registration of a 1/100 of an SLC pixel results in a significant effect that can be used to determine residual co-registration errors very accurately. For this we consider the overlap region between sub-sequent bursts. While the phase match if the co-registration is perfect this is not the case if with a small azimuth mis-registration. In the case of a small mis-registration a constant phase offset is expected. This phase offsets relates linearly to the corresponding azimuth co-registration error. Therefore, it is possible to determine this phase offset and convert it to an azimuth offset correction for the co-registration transformation. To determine such a phase offset coherence in the burst overlap region is necessary. Furthermore, the offset should be determined quite accurately. Therefore, it is best if all burst overlap regions are analyzed to determine a “best global” phase offset and related azimuth offset correction.

This procedure is supported by the program S1_coreg_overlap that estimates an azimuth offset correction based on the phase difference between the two interferograms that can be calculated for the overlap region between subsequent bursts

S1_coreg_overlap SLC1_tab RSLC2_tab 20141003_20141015 20141003_20141015.off
20141003_20141015.off.corrected 0.8 0.01 0.8 1

Figure 15 shows an example of a double difference interferogram used, the related coherence mask and the histogram of the double difference phase for this overlap region. Similarly, all other overlap regions are analyzed to get a “best global azimuth offset correction” estimation.

double difference interferogram (1 color cycle corresponds to 1 phase cycle)

high coherence mask applied

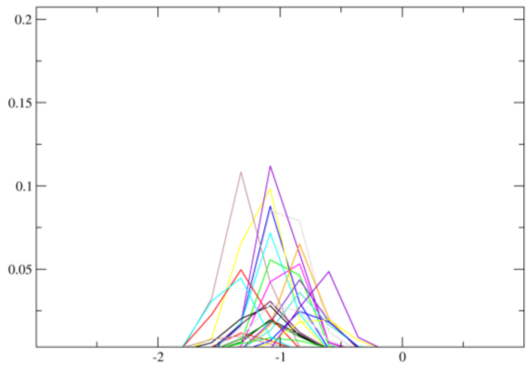

radian

Figure 15 double difference interferogram example (top left), the related coherence mask (bottom left) and the phase difference histograms (right) for all burst overlap regions.

In this method double difference interferograms are generated for all burst overlap regions. The double difference interferograms are multi-looked and unwrapped. To reduce effects from low coherence areas only pixels with coherence values above an indicated threshold are considered. This threshold can be indicated on the command line of *S1_coreg_overlap*. Only overlap regions with a minimal coverage with high coherence pixels are considered (e.g. 0.8). The minimum fraction threshold used can again be indicated on the command line (e.g. 0.01). Then we also consider the statistics of the unwrapped phases. If the standard deviation of the unwrapped phases for a given burst overlap region is larger than an indicated threshold (e.g. 0.8 radian) then the average value determined for this overlap region is not considered, as it is most likely affected by unwrapping errors. The accepted values are then combined using a weighted averaging.

Intermediate files generated by *S1_coreg_overlap* are deleted (as it generates a large number of files for each burst overlap region). Nevertheless, it is possible to keep these intermediate files and investigate why a co-registration failed or how thresholds may be modified to improve the result.

The azimuth offset correction is used to write out a corrected offset parameter file containing the total corrections (20141003_20141015.off.corrected).

We use this corrected offset (*20141003_20141015.off.corrected*) to resample again the S1 TOPS SLC slave with SLC_interp_lt_S1_TOPS

> *SLC_interp_lt_S1_TOPS SLC2_tab 20141015.slc.par SLC1_tab 20141003.slc.par 20141015.slc.mli.lt_fine 20141003.slc.mli.par 20141015.slc.mli.par 20141003_20141015.off.corrected RSLC2_tab 20141015.rslc 20141015.rslc.par*

And again we can optionally check the differential interferogram. We expect to see reduced phase jumps between the bursts.

In the case we still see phase jumps we iterate this spectral diversity method to further improve the co-registration until the phase jumps are no longer visible (typically one iteration is enough). Alternatively, we may also try a manual correction of the azimuth offset if the phase jumps are still visible and the methods fail to automatically determine the necessary correction.

An iteration of the spectral diversity method consists of the estimation of the azimuth offset correction using *S1_coreg_overlap*, and the application of the corrected offset file in the slave burst SLC resampling using *SLC_interp_lt_S1_TOPS*:

> *S1_coreg_overlap SLC1_tab RSLC2_tab 20141003_20141015 20141003_20141015.off 20141003_20141015.off.corrected 0.8 100*

> *SLC_interp_lt_S1_TOPS SLC2_tab 20141015.slc.par SLC1_tab 20141003.slc.par 20141015.slc.mli.lt_fine 20141003.slc.mli.par 20141015.slc.mli.par 20141003_20141015.off.corrected RSLC2_tab 20141015.rslc 20141015.rslc.par*

After a first iteration the azimuth correction found reduced to 0.000269 azimuth SLC pixel and the calculated differential interferogram no phase jumps were visible (Figure 16).

An important output of *S1_coreg_overlap* is the quality information it provides. For the double difference interferograms it provides information on the area that could be used and unwrapped, as well as the per burst overlap region average and standard deviation of the coherence and phase.

In the spectral diversity azimuth offset refinement high enough coherence for some of the burst overlap regions is required to get reliable estimates. In order to increase the chance to find sufficient coherence it is possible to indicate an already co-registered slave that is then used to calculate the double difference interferograms. Here an example: we work with a reference in Oct 2014. We succeed in co-registering scenes until Feb. 2015 to this reference but then the coherence gets too low. So to co-register a reference in 2015 we indicated in RSLC1_tab the reference scene, then in RSLC2_tab the not yet perfect co-registered march 2015 scene and in RSLC3_tab an already well co-registered Feb- 2014 scene. Thanks to the high Feb. to Mar. coherence the spectral diversity method will then reliably work.

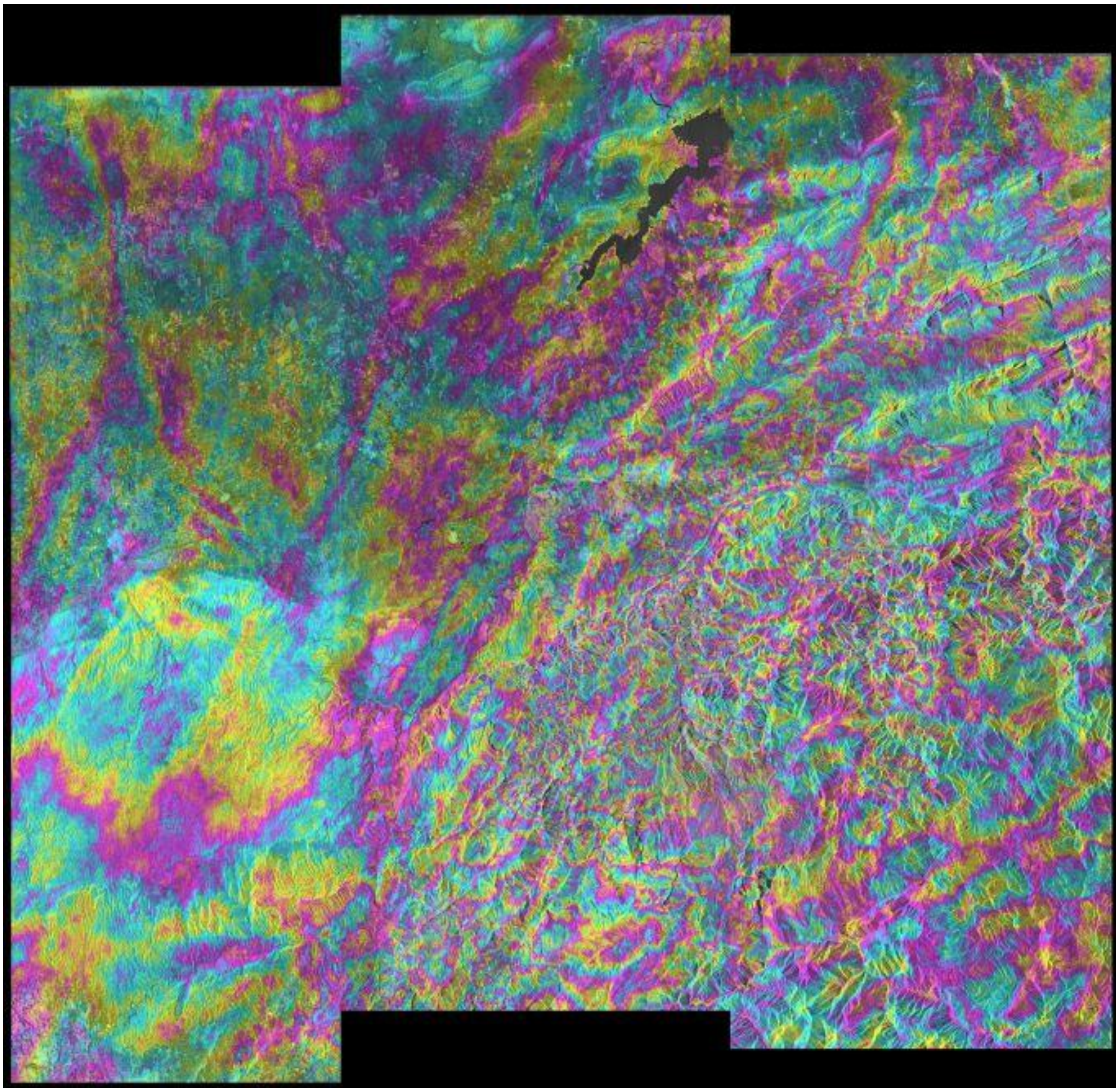

Figure 16 S1 TOPS differential interferogram as obtained after one iteration of the spectral diversity co-registration refinement. One color cycle corresponds to one phase cycle. No more phase jumps are visible at the burst interfaces. The phase matches also well between adjacent sub-swaths.

6.2. TOPS SLC co-registration using script S1_coreg_TOPS

The main steps of the of S1 TOPS SLC co-registration procedure described in Section 6.1 are the calculation of a co-registration lookup table based on the orbit geometry and terrain height and refinements of this lookup table using the intensity matching and the spectral diversity methods. The script *S1_coreg_TOPS* automates this entire procedure. In this it iterates the matching refinement until the azimuth correction determined is < 0.01 pixel. After reaching this quality it iterates the spectral diversity method until the azimuth correction determined is < 0.0005 pixel. An example command is given below

S1_coreg_TOPS 20150308.SLC_tab 20150308 20150320.SLC_tab 20150320 20150320.RSLC_tab 20150308.hgt 10 2 20150308.mask.poly1 20150308.mask.poly2 0.6 0.02 0.8 1 0

As one important output a file containing quality information is generated. This file provides information on the (iterative) co-registration refinements done, first using intensity matching and then using the spectral diversity method (see below).

```
Sentinel-1 TOPS coregistration quality file
############################################
Wed Jun 10 17:54:58 CEST 2015

reference: 20150308 20150308.rslc 20150308.rslc.par 20150308.SLC_tab
slave:     20150320 20150320.slc 20150320.slc.par 20150320.SLC_tab
coregistered_slave:     20150320 20150320.rslc 20150320.rslc.par 20150320.RSLC_tab
polygon used for matching (poly1):          20150308.mask.poly1
polygon used for spectral diversity (poly2):  20150308.mask.poly2

Iterative improvement of refinement offset using matching:
matching_iteration_1: 0.01287 0.05140    0.006435 0.005140 (daz dr   daz_mli dr_mli)
matching_iteration_stdev_1: 0.0232 0.0242 (azimuth_stdev range_stdev)
matching_iteration_2: 0.00292 0.01022    0.001460 0.001022 (daz dr   daz_mli dr_mli)
matching_iteration_stdev_2: 0.0227 0.0228 (azimuth_stdev range_stdev)

Iterative improvement of refinement offset azimuth overlap regions:
az_ovr_iteration_1: -0.000596 (daz in SLC pixel)
20150308_20150320.results
thresholds applied: cc_thresh: 0.6,  ph_fraction_thresh: 0.01, ph_stdev_thresh (rad): 0.8

IW  overlap  ph_mean ph_stdev ph_fraction   (cc_mean cc_stdev cc_fraction)    weight
IW1 1 2.031811e-01 5.303210e-02 0.290369 (9.105916e-01 1.429129e-02 0.298875) 12.398958
IW1 2 5.779061e-02 5.409742e-02 0.281286 (8.755800e-01 1.573436e-02 0.292676) 11.845609
IW1 3 -1.536909e-01 5.726218e-02 0.275952 (8.658296e-01 1.371398e-02 0.288062) 11.157964
IW1 4 1.371792e-01 4.258586e-02 0.279123 (8.971550e-01 9.184040e-03 0.284458) 13.729120
IW1 5 3.265311e-02 3.617400e-02 0.244377 (9.118369e-01 1.008285e-02 0.248847) 13.178681
IW1 6 -8.573833e-02 2.054918e-02 0.242070 (9.330462e-01 1.154657e-02 0.246540) 16.657601
IW1 7 -5.034297e-02 5.029138e-02 0.317618 (9.098332e-01 1.408722e-02 0.330738) 14.061672
IW1 0.021943
IW2 1 2.888122e-02 5.053957e-02 0.267293 (8.767368e-01 3.027912e-02 0.294882) 11.794682
IW2 2 1.779595e-01 1.431418e-02 0.294782 (9.543985e-01 2.290464e-03 0.294882) 22.558008
IW2 3 6.774033e-02 2.937951e-02 0.254298 (8.928206e-01 3.710982e-02 0.283087) 15.191895
IW2 4 -1.705403e-01 3.811974e-02 0.256297 (8.575273e-01 3.768768e-02 0.283087) 13.434825
IW2 5 2.055839e-01 2.414899e-02 0.251200 (8.750782e-01 4.975057e-02 0.283087) 16.297960
IW2 6 1.577327e-01 3.208555e-02 0.275190 (9.341695e-01 9.442051e-03 0.283087) 15.773281
IW2 7 -1.074763e-01 2.950343e-02 0.280088 (9.374377e-01 8.338414e-03 0.283087) 16.700596
IW2 0.052493
IW3 1 -1.383374e-01 2.056179e-02 0.247516 (9.307507e-01 5.570899e-03 0.249951) 17.028794
IW3 2 6.959809e-02 4.781000e-02 0.221313 (8.157243e-01 5.086430e-02 0.266413) 10.129763
IW3 3 3.229673e-01 3.143728e-02 0.196279 (8.310528e-01 7.060535e-02 0.242938) 11.361527
IW3 4 -2.473544e-01 4.588955e-02 0.176018 (8.059804e-01 7.482817e-02 0.222482) 8.270061
IW3 5 1.439114e-02 2.315808e-01 0.143191 (6.497600e-01 4.287495e-02 0.216540) 1.302378
IW3 6 1.452775e-01 9.585197e-03 0.233587 (9.660146e-01 1.379210e-03 0.233587) 19.451132
IW3 7 7.136490e-02 1.835746e-02 0.249854 (9.476542e-01 2.554444e-03 0.250146) 17.835900
IW3 0.037364
all 0.037109
azimuth_pixel_offset -0.000596 [azimuth SLC pixel]

Generated differential interferogram 20150308_20150320.diff
to display use:   eog 20150308_20150320.diff.ras &

end of S1_coreg_TOPS
Wed Jun 10 19:09:15 CEST 2015
```

In such a co-registration process the slave IWS SLC is resampled several times to the master geometry. Such resampling can be significantly accelerated if it is done only for a small section of the entire scene. To limit the area (resampled and) used for the intensity matching refinement iterations a polygon area (*20150308.mask.poly1)* can be indicated. In the case the LAT programs are available only the data of this area is then resampled for the intensity matching refinement iterations. Similarly, the program *S1_poly_overlap* is used (within the program *S1_coreg_TOPS*) to only resample the burst overlap areas when doing the co-registration refinement iterations using the spectral diversity method.

Furthermore, a second polygon area (*20150308.mask.poly2)* can be indicated to restrict the use of the spectral diversity method to suited areas. This can be used to exclude incoherence areas (e.g. ocean) as well as areas with significant movement in azimuth direction (for areas with significant movement in azimuth direction phase offsets not related to the co-registration are expected).

Polygon areas can be defined using the LAT program

*polyras *.ras* > *20150308.mask.poly2*

Without LAT programs *S1_coreg_TOPS* ignores the indicated polygons and does the resampling for the entire area.

6.3. TOPS SLC Interferometry

The main challenge in the S1 TOPS interferometry is the solution of the co-registration (see Sections 6.1, 6.2). Having solved this the perfectly co-registered burst SLC and SLC mosaic pairs are available.

Using the perfectly co-registered burst SLC and SLC mosaic pairs the normal programs for interferometry can be used. The differential interferogram is calculated using the co-registered master and slave mosaic SLCs using the normal approach of the gamma software (with *phase_sim_orb* and *SLC_diff_intf*):

phase_sim_orb 20141003.slc.par 20141015.slc.par 20141003_20141015.off 20141003.hgt 20141003_20141015.sim_unw 20141003.slc.par - - 1 1

SLC_diff_intf 20141003.slc 20141015.rslc 20141003.slc.par 20141015.rslc.par 20141003_20141015.off 20141003_20141015.sim_unw 20141003_20141015.diff.test1 10 2 0 0 0.2 1 1

In the interferogram calculation we can apply range common band filtering but we don’t apply azimuth common band filtering (as the Doppler variations are not represented in the SLC mosaic parameter file).

Phase filtering (e.g. using *adf*), phase unwrapping (using *mcf* or region growing) can be applied as for “normal interferograms”. The coherence can also be estimated in the same way as for “normal interferograms”. The geocoded differential interferogram and the corresponding RGB composite of the coherence (red), the backscatter (green) and the backscatter change (blue) is shown in Figure 17 (overview) and in Figure 18 (smaller section to see possible discontinuities between bursts and sub-swaths.

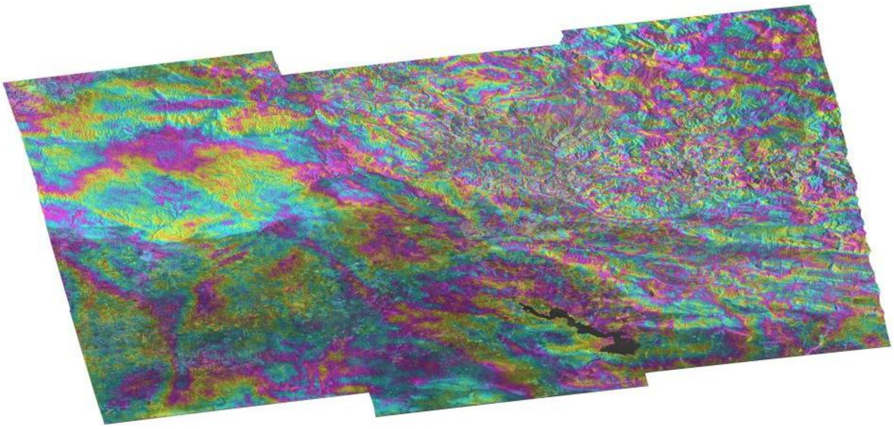

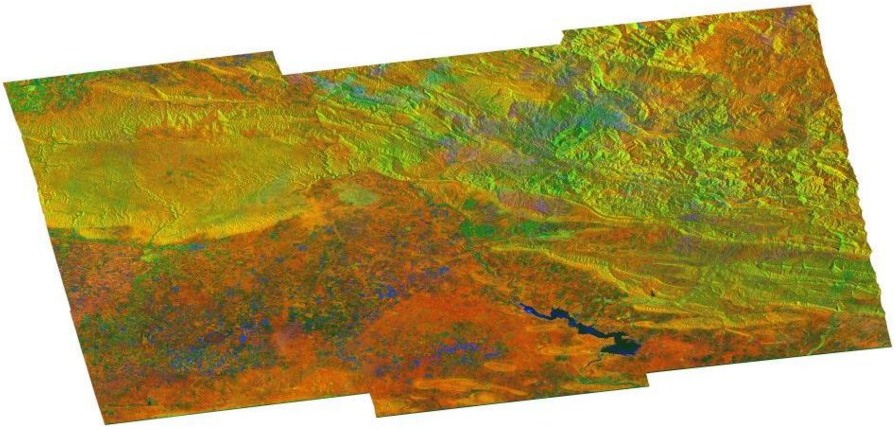

Figure 17 Geo-referenced S1 TOPS differential interferogram (top) and RGB composite (bottom). In the differential interferogram One color cycle corresponds to one phase cycle. No phase jumps are visible at the burst interfaces. The phase matches also well between adjacent sub-swaths.

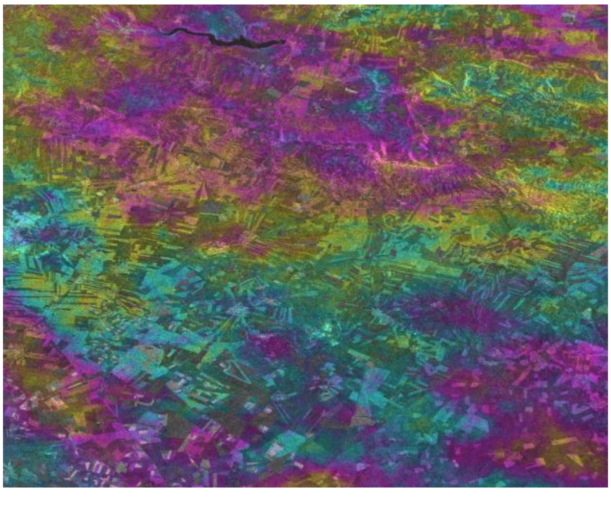

Figure 18 Section (that includes data from two different bursts and two different sub-swaths) of geo-referenced S1 TOPS differential interferogram (left) and RGB composite (right). In the differential interferogram One color cycle corresponds to one phase cycle. No phase jumps are visible at the burst interfaces. The phase matches also well between adjacent sub-swaths. No discontinuities in the coherence are observed.

Most likely along with a processor change on ESA side we noticed in some interferograms a significant phase offsets between IW1 and IW2 while no phase offset between the bursts of one sub-swath were observed. The related interferograms can be corrected by applying a phase offset to the IW1 SLC data. To determine the phase offset the program *S1_coreg_subswath_overlap* can be used (considering in the output the average phase offset between IW1 and IW2). This offset can then be corrected in the IW1 SLC data of the master or the slave. This anomaly only affects pairs with one scene acquired before and one after the change (around 15-Mar-2015).

7. S1 TOPS-mode Persistent Scatterer Interferometry (PSI)

7.1. Basic PSI strategy

An important step in PSI processing using S1 TOPS mode data is (as for interferometry in general) the very careful co-registration of the burst SLC. For this the procedure and tests as described in Section 6.1 can be used.

Then the basic strategy is to deramp all the burst SLC using for all co-registered burst SLC the identical phase ramp, which is the one determined for the master scene. Using the deramped burst SLC stack a deramped SLC mosaic stack is generated. This stack is then used as input to the PSI processing in the same way as “normal data”.

To deramp the reference burst SLC the program *S1_deramp_TOPS_reference* can be used. For the reference scene it calculates the deramped burst SLC as well as the deramp phases used. These deramp phases can then be applied to slave burst SLCs that are co-registered to this master using the program *S1_deramp_TOPS_slave*.

For the deramped burst SLCs SLC mosaics are generated.

This stack of deramped co-registered mosaic SLCs is then used as input to the PSI processing in the same way as “normal data”.

The spectral diversity method (using *sp_stat* program) can be used in this way (because of the deramping of the SLCs). Range oversampling of the SLCs can also be applied if the SLCs were deramped.

Considering the good range resolution a relatively high number of suited persistent scatterers is expected.

Considering the large areas covered applying the available advanced techniques to optimally reduce the point densities seems very appropriate. The fact that only the vector data stacks are used in most IPTA programs means that the relevant parameter for the speed of a processing step is not the size of the area or of the full SLC but only the number of points in the point candidate list. This makes the IPTA approach very efficient for S1 PSI.

An example of a result as presented in March 2015 [6] is shown in Figure 19. Figure 20 shows the result for the full point list and a reduced point candidate list initially used in the development of the solution. For more details on this processing and a comparison with an SBAS style processing it is referred to [6].

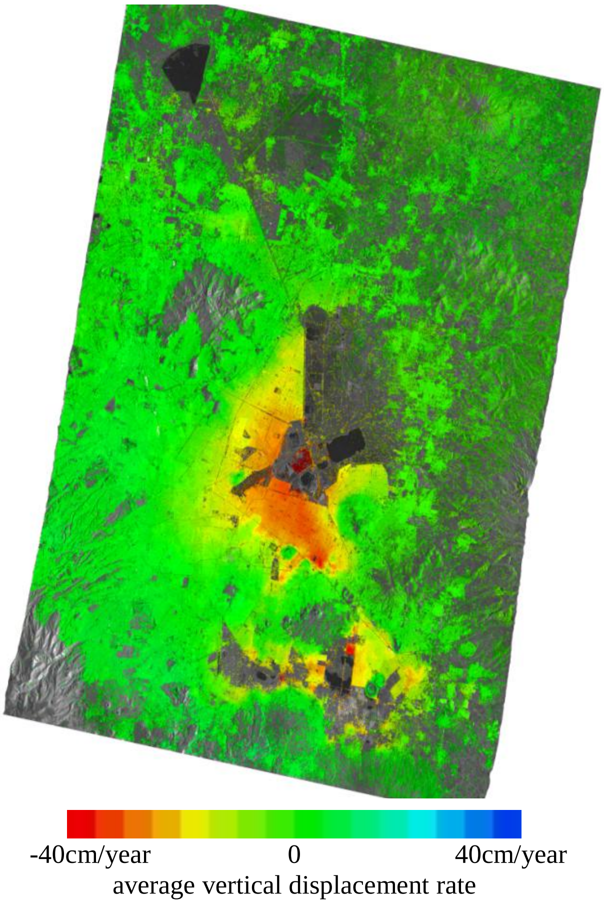

Figure 19 Average vertical displacement rate derived from a stack of 12 S1 IWS SLC over Mexico City using a PSI procedure (color scale is indicated above to the right).

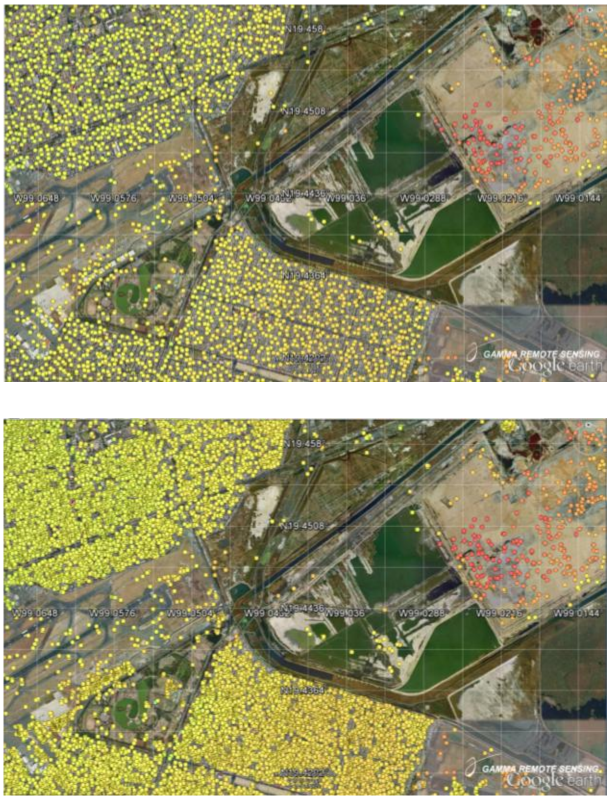

Figure 20 Local visualization of the S1v IWS PSI result over Mexico City (LOS displacement rates) in Google Earth with reduced (top) and full (bottom) point density.

7.2. Investigating burst overlap regions

In the approach described in Section 7.1 only data of one burst is considered in the burst overlap (and sub-swath overlap) regions. This seems very reasonable as it results spatially in more consistent point densities etc.

To specifically investigate how points behave in the two different bursts (or sub-swaths) of an overlap area the programs to extract SLCs of single bursts can be used.

8. S1 TOPS-mode Offset Tracking

8.1. Basic offset tracking strategy

To apply offset tracking for S1 TOPS mode SLC data the basic strategy is to first co-register the two burst SLC as described in Sections 6.1 and 6.2. In this it may be a good idea to mask areas with significant azimuth displacements as these will affect the co-registration refinement using the spectral diversity method (see Section 6.2). Then, considering that (1) the oversampling is recommended in the offset tracking procedures to optimize the quality of the estimated offsets and (2) that the SLC oversampling applied in the offset matching programs (offset_pwr, offset_pwr_tracking) we first deramp the master:

echo 20141003.IW1.slc.deramp 20141003.IW1.slc.deramp.par 20141003.IW1.slc.deramp.TOPS_par" > SLC1_tab.deramp

echo 20141003.IW2.slc.deramp 20141003.IW2.slc.deramp.par 20141003.IW2.slc.deramp.TOPS_par" >> SLC1_tab.deramp

echo 20141003.IW3.slc.deramp 20141003.IW3.slc.deramp.par 20141003.IW3.slc.deramp.TOPS_par" >> SLC1_tab.deramp

SLC_deramp_S1_TOPS SLC1_tab SLC1_tab.deramp 0 1

In this step we write out the phase ramps used (*20141003.IW1.slc.deramp.dph 20141003.IW2.slc.deramp.dph 20141003.IW3.slc.deramp.dph*) for the deramping and apply the identical phase ramp (of the master) to the co-registered slave burst SLC :

create_diff_par 20141003.IW1.slc.par - 20141003.IW1.slc.diff_par 1 0

create_diff_par 20141003.IW2.slc.par - 20141003.IW2.slc.diff_par 1 0

create_diff_par 20141003.IW3.slc.par - 20141003.IW3.slc.diff_par 1 0

sub_phase 20141015.IW1.rslc 20141003.IW1.slc.deramp.dph 20141003.IW1.slc.diff_par 20141015.IW1.rslc.deramp 1 0

sub_phase 20141015.IW2.rslc 20141003.IW2.slc.deramp.dph 20141003.IW2.slc.diff_par 20141015.IW2.rslc.deramp 1 0

sub_phase 20141015.IW3.rslc 20141003.IW3.slc.deramp.dph 20141003.IW3.slc.diff_par 20141015.IW3.rslc.deramp 1 0

For the deramped master and slave burst SLC we generate the corresponding SLC mosaics:

echo "20141015.IW1.rslc.deramp 20141003.IW1.slc.deramp.par 20141003.IW1.slc.deramp.TOPS_par" > RSLC2_tab.deramp

echo "20141015.IW2.rslc.deramp 20141003.IW2.slc.deramp.par 20141003.IW2.slc.deramp.TOPS_par" >> RSLC2_tab.deramp

echo "20141015.IW3.rslc.deramp 20141003.IW3.slc.deramp.par 20141003.IW3.slc.deramp.TOPS_par" >> RSLC2_tab.deramp

SLC_mosaic_S1_TOPS SLC1_tab.deramp 20141003.slc.deramp 20141003.slc.deramp.par 10 2

SLC_mosaic_S1_TOPS SLC2_tab.deramp 20141015.rslc.deramp 20141015.rslc.deramp.par 10 2

Alternatively we can use the scripts *S1_deramp_TOPS_reference* and *S1_deramp_TOPS_slave* (see also Section 7.1). For the deramped burst SLCs SLC mosaics are generated.

The deramped mosaic SLCs are then used for the offset tracking

create_offset 20141003.slc.deramp.par 20141015.slc.deramp.par 20141003_20141015.off 1 10 2 0 *offset_pwr_tracking 20141003.slc.deramp 20141015.rslc.deramp 20141003.slc.deramp.par 20141015.rslc.deramp.par 20141003_20141015.off 20141003_20141015.offs 20141003_20141015.snr 100 20 - 2 5.0 40 8 - - - - 4 0*

Because of the deramping we can now indicate an SLC oversampling factor larger than 1 (here 2). Further processing (quality control, geocoding, conversion to displacements in meters, visualization) is done as for normal stripmap mode data.

The main interest in offset tracking is to map displacements. An example of a glacier velocity map over a part of Greenland is shown in Figure 21. As compared to ENVISAT ASAR the sensitivity is improved in range direction thanks to the higher S1 range resolution. On the other hand the resolution is lower in azimuth direction as a consequence of the lower azimuth resolution of the IWS data. Besides, azimuth offsets may also be of interest to identify ionospheric effects [1]. An example of an azimuth offset field over Devon Ice Cap, Canada, clearly affected by ionospheric effects is shown in Figure 21.

8.2. Investigating burst overlap regions

Investigating offsets in the burst overlap regions may be of interest e.g. to investigate ionospheric effects which are potentially different for the two overlapping bursts because of the different squint used. Such processing can be done e.g. by copying out individual bursts into separate SLCs.

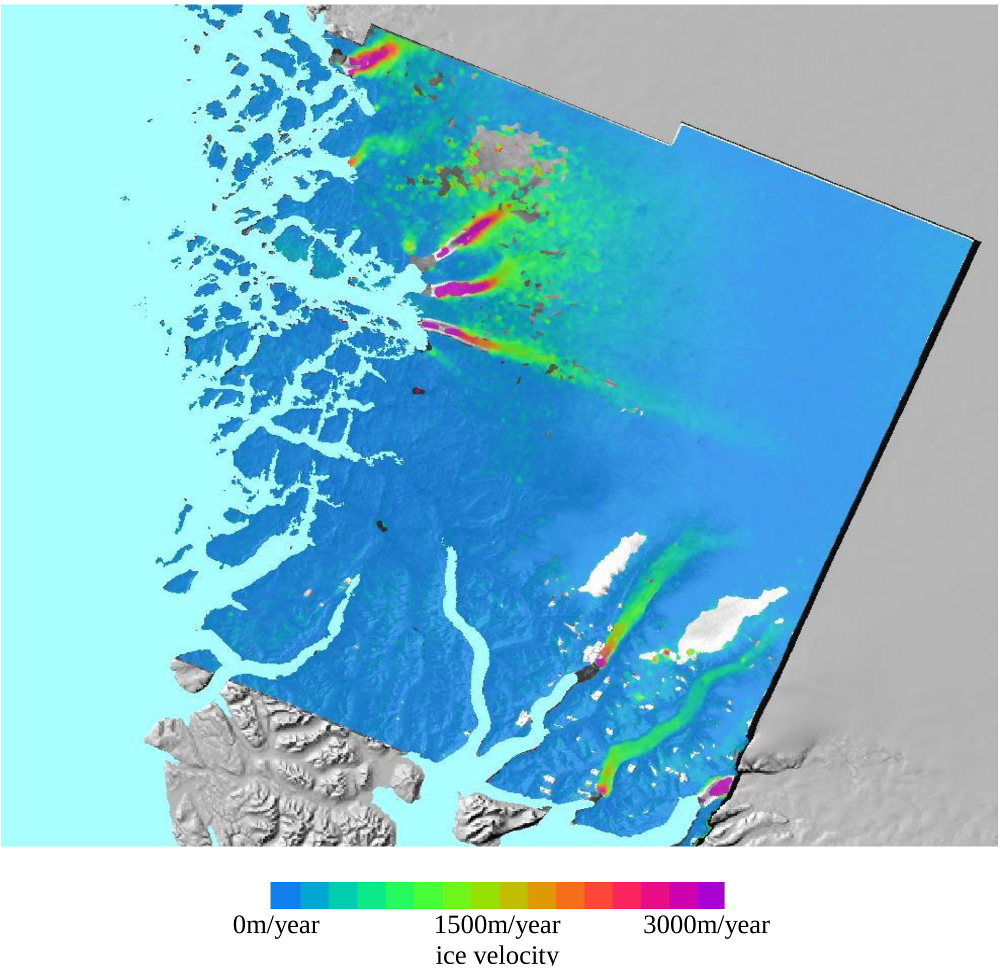

Figure 21 Velocity map of the Upernvaik area overlayed the shaded relief of the Greenland Mapping Project (GIMP) DEM [7]. Image width is about 250 km.

9. S1 TOPS-mode Split-Beam Interferometry

9.1. Split-beam interferometry within bursts

Split-beam interferometry, SBI, (or multi-aperture interferometry, MAI) can be applied to the S1 TOPS SLC data. For this the SLC are first co-registered (as shown in Sections 6.1 and 6.2) and the azimuth spectra are deramped (as shown in Section 8.1). The deramped mosaic SLC can be used for SBI in the same way as normal strip-map mode data, e.g. using the script SBI_INT:

SBI_INT 20141003.slc.deramp 20141003.slc.deramp.par 20141015.rslc.deramp 20141015.rslc.deramp.par 20141003_20141015.sbi_int 20141003_20141015.sbi_int.off 20141003_20141015.sbi_pwr 20141003_20141015.sbi_pwr.par 0.5 10 2

Notice that the azimuth bandwidth is small and therefore the spectral separation of the two sub-bands limited. It is recommended to check the spectra of the two co-registered deramped mosaic SLC to determine the suited azimuth sub-bands to use.

Another relevant point to notice is that an azimuth co-registration error will introduce a phase offset because of the azimuth phase ramp related to the Doppler Centroid variation within each burst.

9.2. Split-beam interferometry between bursts

In the co-registration procedure described in Section 6.1 the SBI in the burst overlap between the different bursts is used to determine the final co-registration refinement in the azimuth direction. As a result of the significant Doppler Centroid difference between the two bursts (one overlap is the beginning of the Doppler ramp the other one the end of the Doppler ramp) there is a good sensitivity to estimate co-registration errors. Besides overall co-registration errors there can also be local co-registration errors caused by along-track motion of the surface (e.g. a north-south flowing glacier) which causes significant phase “anomalies” in the split-beam interferogram that can be considered to retrieve displacement information. Nevertheless, this method can only be applied for the burst overlap areas – which are small.

SBI within or between bursts may also be of interest to identify ionospheric effects [2]. An split-beam interferogram example over Devon Ice Cap, Canada, clearly affected by ionospheric effects, is shown in Figure 22.

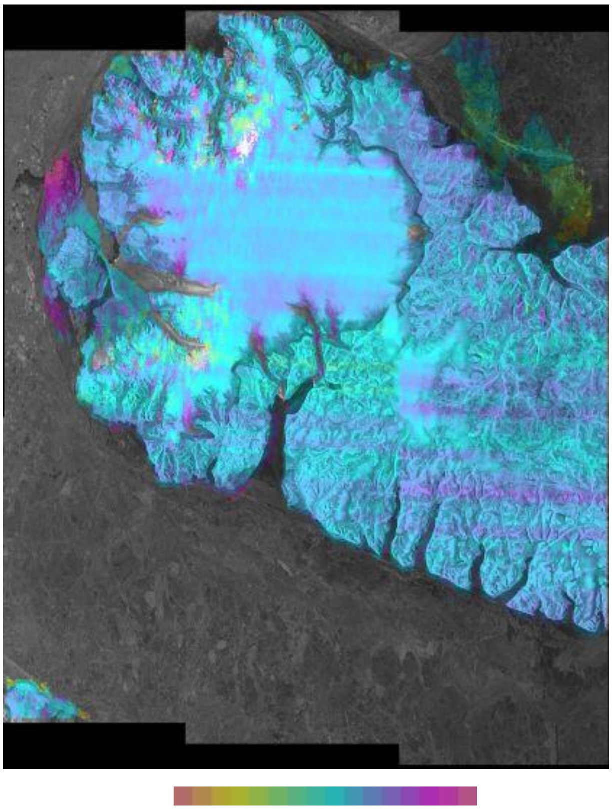

-0.2 0 +0.2

azimuth offset in SLC pixel

Figure 22 Devon Ice Cap, Canada. Azimuth offsets between S1 IWS data of 20150117 and 20150129 showing “ionospheric azimuth streaking” of the order of 0.1 SLC pixel.

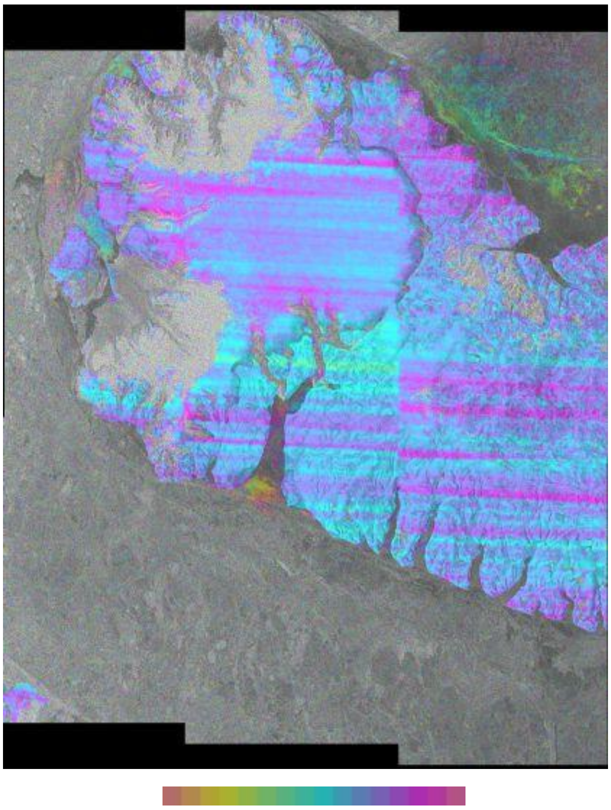

-0.5rad 0 +0.5rad

SBI phase in radian

Figure 23 Devon Ice Cap, Canada. Split beam interferometric phase of S1 IWS pair of 20150117 and 20150129 showing “ionospheric azimuth streaking” of the order of 0.5 radian.

10. Adding OPOD precision state vectors

Some days after the acquisition ESA provides for S1 data access to precision state vectors (online at https://qc.sentinel1.eo.esa.int/aux_poeorb/). These precision state vectors can be read and copied to the SLC parameter files using the program *S1_OPOD_vec*. Overall we find that the quality of the state vectors provided with the S1 SLC and GRD data products is already high and sufficient for geocoding, co-registration and interferometry. Nevertheless, especially in the case of anomalous results it is highly recommended to use the state vectors OPOD precision state vectors.

For concatenated scenes the state vectors available with the date need to be interpolated to one on common time sampling grid. This requires interpolation which can slightly degrade the quality of the state vectors. So using the OPOD precision state vectors is preferred reliable solution.

11. References

[1] Wegmüller U., C. Werner, T. Strozzi, and A. Wiesmann, “Ionospheric electron concentration effects on SAR and INSAR”, Proc. IGARSS 2006, Denver, Colorado, USA, 31- Jul. – 4. Aug. 2006.

[2] Wegmüller U., T. Strozzi, and C. Werner, Ionospheric path delay estimation using split-beam interferometry, Procs. IGARSS‘2012, Munich, Germany, 22-27 July 2012.

[3] De Zan F. and A. Guarnieri, Terrain Observation by Progressive Scans, IEEE Trans. Geosci. Remote Sensing, vol. 44, no. 9, pp. 2353-2360, 2006.

[4] Prats P., L. Marotti and R. Scheiber, Investigation on TOPS Interferometry with TerraSAR-X, Proc. of IGARSS 2010.

[5] Scheiber R. and A. Moreira, Coregistration of interferometric SAR images using spectral diversity, IEEE Trans. Geosci. Remote Sensing, vol. 38, no. 5, pp. 2179–2191, 2000.

[6] Wegmüller U., C. Werner, T. Strozzi, A. Wiesmann, O. Frey, and M. Santoro, "Sentinel-1 support in the GAMMA Software", Procs Fringe 2015 Conference, ESA ESRIN, Frascati, Italy, 23-27 Mar. 2015

[7] Howat, I.M., A. Negrete, B.E. Smith, 2014, The Greenland Ice Mapping Project (GIMP) land classification and surface elevation datasets, *The Cryosphere*, 8, 1509-1518, doi:10.5194/tc-8-1509-2014.